UNIVERSITY OF KWAZULU-NATAL ™

INYUVESI YAKWAZULU-NATALI

OPTIMIZATION OF THE NATURAL FREQUENCY OF HYBRID, MULTI-SCALE GRAPHENE/FIBRE REINFORCED NANOCOMPOSITE LAMINATES

By:

Yajur Jeawon

In fulfilment of the Master of Science in Civil Engineering, the College of Agriculture, Engineering and Science, University of Kwa-Zulu Natal

Date:

23 April 2020

Name & Student Number:

Yajur Jeawon - 211558010

Supervisor:

Dr G. A. Drosopoulos

Examiner's Copy

DECLARATION - PLAIGERISM

I, Yajur Jeawon, declare that:

1. The research reported in this thesis, except where otherwise indicated, is my original research.
2. This thesis has not been submitted for any degree or examination at any other university.
3. This thesis does not contain other persons' data, pictures, graphs or other information, unless specifically acknowledged as being sourced from other persons.
4. This thesis does not contain other persons' writing, unless specifically acknowledged as being sourced from other researchers. Where other written sources have been quoted, then their words have been re-written but the general information attributed to them has been referenced

b. Where their exact words have been used, then their writing has been placed in italics, inside quotation marks, and referenced.

5. This thesis does not contain text, graphics or tables copied and pasted from the Internet, unless specifically acknowledged, with the source being detailed in the thesis and in the references sections.

Signed:

……

As the candidate's supervisor, I agree to the submission of this thesis.

Signed:

……

DECLARATION - PUBLICATION

This thesis has been created with the contribution of the following co-authors, which are about to participate in the publication: Yajur Jeawon, Georgios A. Drosopoulos, Georgia-Ntora Foutsitzi, Georgios Stavroulakis and Sarp Adali.

Dr. Georgios A. Drosopoulos is the supervisor of this masters research. Professor Georgia-Ntora Foutsitzi provided the finite element analysis code, contributed by advice and discussions on the research. Professor Georgios Stavroulakis provided the optimization code, contributed to the research by several discussions and advice on the topic. Professor Sarp Adali provided advice and discussions on the topic.

Yajur Jeawon combined the tools which have initially been sent independently (one finite element analysis Matlab code and one optimization Matlab code) into a unique, holistic Matlab code, elaborating optimization and the finite element analysis for graphene nanocomposite materials. Using this concept, he conducted the research regarding the topic to build an introduction, motivation and research methodology as well as the literature review. He then went on to use the Matlab code to simulate each test, producing results in an appropriate manner by tables and figures. Yajur then analysed these results and produced a discussion and conclusion to the thesis.

TABLE OF CONTENTS

LIST OF TABLES

LIST OF FIGURES

ACKNOWLEDGEMENTS

I would like to achkowledge those who made it possible to complete this research:

- Dr GA Drosopoulos for his constant inspiration, encouragement and supervision throughout the research period.
- Professor Georgia-Ntora Foutsitzi, Professor Georgios Stavroulakis and Professor Sarp Adali who aided and supported my research.
- My parents and brothers for giving me the courage and strength to continue my studies.
- Dr A. Singh for the never-ending love and support that helped me stay focussed and progress.

OPTIMIZATION OF THE NATURAL FREQUENCY OF HYBRID, MULTI-SCALE GRAPHENE/FIBRE REINFORCED NANOCOMPOSITE LAMINATES

Abstract

The optimal solution of the natural vibration problem is investigated in this thesis, for a hybrid, multi-scale graphene/fibre reinforced composite laminate plate. Although several research outputs have been published on the optimization of traditional fibre reinforced composites, the investigation of the reinforcement of these composites by adding a nanomaterial, is still an open topic. The fundamental frequency is optimized within a Sequential Quadratic Programming algorithm. Micromechanics equations are used to produce the effective material properties of the 3-phase laminate plate and finite element analysis is adopted to derive the natural frequencies. Several design variables are considered in the optimization problem, emphasizing in the influence of graphene nanoplatelets' weight on the optimal vibration response. Results indicate the optimal distribution of graphene in the laminate for several stacking sequences, boundary conditions and different fibre types (glass or carbon). It is shown that a non-uniform distribution of graphene along the layers of the laminate, results in optimal vibration response. The boundary conditions, as well as the type of fibres (glass or carbon) also affect significantly the natural frequencies.

Keywords: graphene nanoplatelets, optimization, natural frequency, multi-scale laminate

CHAPTER 1: INTRODUCTION

1.1 Background

The evolution of materials and components in various industries has been a core ideology in the improvement of society. The combinations of various materials to produce composites, that surpass the individual properties of the parent elements, have been key in the advancement of technology.

Industries such as automotive, aerospace and construction have utilized high-performance light-weight composite materials to produce exciting, new innovations that were once thought of as impossible. [1]

The addition of nanoparticles to these composite materials makes it possible to substantially improve the mechanical properties, electrical conductivity, natural frequency, thermal stability and chemical resistance etc. whilst allowing the advantageous characteristics of the parent material such as low density and high processability to be preserved. [2]

The design of structures such as aircrafts and spacecrafts require thin plates which makes vibrations in the structure important. Decreasing the thickness lowers the fundamental frequency. Due to the fact that continuous fibre reinforced plates are required to have high strength and stiffness, these plates should be designed to be as thin as possible. Increasing the thickness of the plate beyond the required strength parameter does not conform to the requirements of a lightweight, cost effective design. The design optimization can be achieved by modifying the material system by means of stacking sequence, fibre orientation, composite composition and material type. This method can optimize the natural frequency without increasing the thickness of the plate thereby providing a lightweight, cost effective design [3].

The focus of this thesis is the optimization of the natural frequency of hybrid, multi-scale graphene/fibre reinforced nanocomposite laminates. Knowledge of the natural frequency of a structure and how to optimize it will significantly influence the proper design and usage of the material. Optimization of the natural frequency, for the scope of this thesis, means designing the laminate for the maximum frequency,

which results in avoiding resonance and succeeding an optimal response against vibration actions [4].

Resonance is a phenomenon experienced when loading frequencies coincide with the natural frequencies of a structure. It is able to induce severe damage to the structure which could cause it to fail. [5]

In aero engines and other rotating machines dynamic forces are experienced in the structure which can cause them to vibrate. These components can already be highly stressed due to their functions or locations in the machine. The increase in vibrations of the system can cause early fatigue damage which is a serious concern. [6]

Therefore, the need arises for a proper design of composite laminate structures against dynamic actions. Significant parameters of this design are the type, quantities and distribution of constituent materials within the laminate. The traditional constituent materials used to compose a laminate are the matrix, which is usually a polymer material and the glass or carbon fibres, which are embedded within the matrix as the reinforcement of the laminate. To further improve the mechanical properties of composite laminates, the idea of incorporating a small quantity of a nano-reinforcement, such as carbon nanotubes or graphene nanoplatelets has been introduced [6]. The superior material properties of the nano-reinforcement compared to traditional fibre reinforcement is expected to result in the improvement of the structural response of the new composite laminate. Since three constituent materials are used: the matrix, the traditional fibres (carbon or glass) and the nano-reinforcement, the terms 3-phase composite or hybrid composite are used in literature for these materials [7].

In [7] it is found that low amounts of graphene platelets perform better than carbon nanotubes with respect to Young's Modulus, tensile strength, fracture toughness, and resistance to fatigue crack growth.

Graphene used as a nano-reinforcement has become an exciting material due to its excellent mechanical characteristics. The optimization of natural frequencies of composite plates due to the addition of graphene is a growing study. More research is required in this topic to develop solid information regarding optimization and the

graphene material. [8] is a study that analysed the natural frequency of a sandwich plate with a graphene platelet (GPL) reinforced face layers.

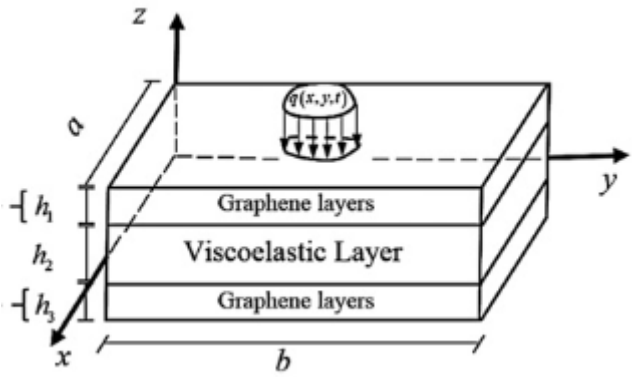

Figure 1.1. 1: Sandwich plate with graphene face layers [8]

The numerical results showed that various types of graphene distributions in the layers increased the natural frequency. The comparison between zero graphene and 1% graphene resulted in a natural frequency of approximately double. The natural frequencies for Pure Epoxy and the 'Outer-rich' graphene distribution were 10.8547(Hz) and 22.4279(Hz) respectively. The study showed the GPL distribution and volume fraction of graphene had remarkable effects on the natural frequencies. The 'outer-rich' distribution which had the most graphene content in the outer layers produced the highest natural frequency. Additionally, applying different GPL distributions to the top and bottom layers resulted in an even higher natural frequency. This study reveals that GPLs have substantial effects on natural frequency therefore studies can be done to highlight the most efficient methods of using GPLs to achieve lightweight, cost-effective nanocomposites.

To increase the natural frequency of a composite, a numerically study is done in this thesis, with respect to the addition of nano-reinforcement within traditional fibre reinforced composites such as glass or carbon fibres. The nano-reinforcement which is chosen as the investigative material in this thesis is made of graphene nanoplatelets. Graphene is among the strongest, thinnest materials on earth. In addition, studies related to optimization of the natural vibration for 3-phase graphene reinforced composites, don't seem to appear in the current literature. Graphene is also an expensive material, indicating that the quantity of it that needs to be used within the laminate, is of major importance. Hence, applications should consider

optimization of the graphene content and distribution along the thickness of the composite, to ensure a cost effective design.

The research presented in this thesis highlights the changes in natural frequency when the composition of the nano-reinforced composite laminate is altered. The quantity of graphene needed to obtain an optimized natural frequency as well as the content of the traditional reinforcement, are among the fundamental parameters that are investigated in this thesis. The results presented can aid further research regarding graphene and its usage within a nanocomposite laminate.

1.2 Research Question

How could the use of graphene as a nano-reinforcment optimize the vibrational response of a composite laminate?

1.3 Aims and Objectives

1.3.1 Aims

- To develop a numerical model of a graphene nano-composite plate
- To conduct studies related to the vibrational response of the material

1.3.2 Objectives

- Simulate the effective material properties of graphene nano-composites;
- Generate numerical models of graphene plates;
- Analyse the vibrational response of graphene plates in static or/and dynamic analysis framework;
- Identify the optimum quantities of graphene and fibre reinforcement and the influence of other parameters on the vibrational response.

1.4 Motivation

To the author's knowledge, it seems that no published work is found to study the optimization problem of the natural frequency of 3-phase, graphene/fibre reinforced composite laminates. Therefore, the goal of this research is to provide information and offer an insight on the vibration response of these laminate composite plates.

The research involves the use of a traditional composite using glass or carbon fibres as reinforcement to the matrix. Graphene platelets (GPLs) are added as nano-reinforcement and varied by means of minimum/maximum limits for each layer, imposing, in some cases, a maximum overall graphene limit for the laminate. Simulations determine the optimum natural frequency of the composite laminate which could be extended to industry applications in various fields such as aerospace.

Composites are widely used in industry. They could be improved by adjusting the materials and quantity of material used to determine the most cost effective solution. Optimizing the natural frequency could assist in reducing the appearance of the resonance phenomenon thereby decreasing the potential damage to the structure. Therefore, this thesis has been undertaken to contribute information regarding the use of graphene to optimize the natural frequency with the hopes of aiding industry advancement.

1.5 Research Methodology

1.5.1 Planning

In the planning stage the concept idea of the research topic was discussed to determine what the relevant testing criteria would be incorporated in the thesis. The design procedure was discussed and researched in detail to ensure the correct procedure was followed to produce the final results.

1.5.2 Literature Review

The literature review involves the analysis of previous data from scientific research papers and journals. The literature provides a background into the topic relating to similar research completed which introduces the research idea, displays the concepts and methods used that will ultimately produce the final results.

1.5.2 Procedure and data analysis

The methods undertaken to complete this research involved the initial study of composite materials from literature to gain knowledge on the applications, structure types, constituent and traditional materials used. The initial study also aided in determining the lack of information on topics.

The composite was selected incorporating a matrix and fibre reinforcement (Glass/Carbon Fibre). The main concern of this thesis involved the use of graphene platelets, as nano-reinforcements, to optimize the composite plate in terms of natural frequency. The effective material properties, which are the average material properties of the composite, were determined from the use of equations acquired from literature to determine the overall properties of the composite laminate.

Matlab was used to generate the optimization function so that simulations could be run for various parametric investigations in the composite laminate. Once the optimization function was finalized and ready to be used, the simulations relating to various changes such as graphene weight, fibre content, fibre angle and others were numerically tested. The results of this were recorded. These results were tabulated and analysed to determine their validity in this research.

CHAPTER 2: LITERATURE REVIEW

2.1 Introduction

Nanocomposite laminates are widely used in several sectors in civil, mechanical and aerospace engineering. The concept of the enhancement of traditional composite structures by utilizing advanced materials with superior mechanical properties has significantly been developed in recent years. Within this framework, recent research efforts have highlighted the idea of incorporating nano reinforcement, such as carbon nanotubes (CNTs) or graphene nanoplatelets (GPLs) in fibre reinforced composites.

Graphene is a monolayer of sp^2 hybridized carbon atoms arranged in a honey comb structure. It is well known for its exceptional mechanical properties such as Young's Modulus 1 Tpa, fracture strength 130 GPa and similar electrical/thermal conductivity to copper [9]. It also possesses additional beneficial properties such as being lightweight with high electrical conductivity and mechanical toughness [10]. It is already used widely in several industrial applications [11, 12].

It has been found that the usage of a 0.54% volume of exfoliated graphene in comparison with a neat resin increased the elastic modulus by 25% and the tensile strength by 10% as seen in [13] showing graphene has potential as a nano-reinforcing material. In [14] tests for the flexural modulus and fracture toughness after the addition of graphene into a resin showed an increase of flexural modulus by 14% and fracture toughness of 28%. When introducing nanocomposite reinforcement into composite laminates consideration must be given to diminishing returns (amount of reinforcement used vs the gain in structural response) as well as to the optimal nanocomposite content which leads to maximum enhancement of the response. Within this framework, several efforts were made to study the behaviour of nano-reinforced laminate structures under vibration, buckling or bending actions. One of the main concepts of the study is the investigation of two-phase graphene reinforced nanocomposite laminates.

Free vibration, buckling and static bending analysis of multilayer functionally graded graphene nanoplatelets (GPLs) reinforced composite plates were analysed in [15]. The Young's Modulus of the nanocomposite was predicted using the modified Halpin-Tsai micromechanical model. The results indicated that the natural frequencies and buckling loads were significantly improved with the addition of graphene. In [16] the vibration damping properties of GPLs reinforced NR/EPDM (Natural rubber / ethylene-propylene-diene rubber) nanocomposites were tested via the free vibration test. The results showed the addition of GPLs significantly improved the damping ratio values (up to 50%) when compared to NR/EPDM blend. The effect of elastic foundations in thermal environments on the nonlinear vibration of functionally graded graphene reinforced composite laminated beams can be seen in [17]. The influence of graphene oxide powder (GOP) on the bending, buckling, and vibration behaviour of functionally graded multilayer nanocomposite beams were studied in [18]. It was stated that GOP is superior to single and multi-walled carbon nanotubes in the reinforcement of polymer nanocomposites. The addition of graphene on temperature-dependent laminates was tested in [19] to determine the natural vibration response.

Light weight structures are often exposed to severe vibration actions. It is, therefore, becoming important to investigate the optimal performance against resonance. The goal of the optimization is to maximize the natural frequency of the structure thereby reducing the likelihood to experience resonance. Physical observation identifies that the outer layer of a composite has a greater stiffening effect than the inner layer in bending, indicating that the outer layer is more influential in determining the natural frequency of the plate [20]. A statistical analysis on free vibration of functionally graded graphene reinforced composite plates can be seen in [21]. The study showed that boundary condition and volume fraction of GPLs were the most significant parameters for the vibration response, followed by thickness ratio and distribution pattern of GPLs. More published research on analysis of two-phase graphene reinforced nanocomposite plates can be found in [22, 23, 24, 25, 26], the results of the investigations have been summarized in Table 2.1.1.

Table 2.1. 1: Analysis of two-phase graphene reinforced nanocomposite plates from [22, 23, 24, 25, 26]

Reference	Investigation	Analysis Result
22	Linear and nonlinear free vibration behaviour of nanocomposite beams, reinforced with GPLs.	• Addition of small amount of GPLs improved structural performance and increased natural frequency of the composite beams
23	Importance of the orientation of the nanoplatelets and strength of the interface with the matrix.	• Aligned nanoplatelets gave approximately twice the level of reinforcement then that of a random distribution.
24	Effect of graphene and graphene dispersion state on fracture toughness.	• Graphene enhances the fracture toughness of epoxy nanocomposites up to 131%. • Uniformly dispersed graphene increased fracture toughness compared to randomly dispersed graphene.
25	Efficiency of graphene based nanocomposites as thermal interface materials.	• The modelling resulted in graphene nanocomposites outperforming carbon nanotube composites and those with metal nanoparticles.
26	Investigation of the free and forced vibration characteristics of functionally graded multilayer graphene nanoplatelets composite plates.	• A small amount of graphene can significantly increase natural frequency. • Dispersing more square shaped GPLs near the top and bottom surfaces of the plate is more effective to increase natural frequency.

Structural modelling of carbon nanotubes and graphene nanoplatelet reinforced laminated composite beams have become a topic of active research in recent years. A structural model for the analysis of 3-phase multi-scale laminated carbon nanotube reinforced composite beams and plates were developed by Rafiee and his co-workers. Studies were carried out in [27, 28, 29, 30, 31, 32, 33, and 34]. Numerical results shown in [27] indicated that the central deflection and natural frequency were significantly improved by incorporating a small percentage of GPLs in multiscale fibre-reinforced composite. [28] concluded that graphene nanoparticle (GNP) volume fraction in the composite had a strong influence on both axial and transverse moduli. The moduli increased with increasing GNPs. The experimental result in [29] showed that addition of GNPs improved the ultimate tensile strength, flexure properties and interlaminar shear strength of the composite. In [30] it was shown that embedding CNTs–GPLs hybrids into pristine epoxy resulted in a significant improvement of the

load transfer effectiveness as well as in great enhancement of the mechanical properties. In [31] a test was done to find out the effect of adding carbon fibres and carbon nanotubes to reinforce a polymer matrix. The conclusion was that the elastic modulus considerably improved with this reinforcement. [32] tested resonant dynamics of carbon nanotube (CNT) multiscale laminated composite rectangular plates. The result shows that increasing the weight percentage of CNTs caused an increase in the frequency of the plate. [33] analysed the natural frequency response of using CNTs in non-uniform multi-scale composite beams. The result indicated the CNT volume fraction does not significantly affect the natural frequency of orthotropic beams with 0° layers. In [34] it was proved that making the outer layers of a laminate thicker than a certain percentage of the total laminate thickness may lead to diminishing returns related to the buckling strength, for increasing fibre content. This means that adding thickness to the outer layers will increase the buckling strength but after the outer layers become approximately 50% thicker than the laminate thickness this increase tapers off. After this point the laminate becomes less cost effective.

Several research efforts have also been conducted on the optimization of traditional, fibre reinforced polymer laminate composites, focussing on buckling and vibration response [20, 35, 36, 37, 38, 39]. However, a relatively small number of efforts have lately been extended to study the response of nanocomposite, multi-scale (two-phase or 3-phase) reinforced polymers. In [40] the optimal solution of natural vibration of carbon nanotubes (CNTs) reinforced polymer beam is investigated. Results indicated that more CNTs volume fraction does not necessarily increase the natural frequency. In [41] the optimal solution of the free vibration problem is studied for 3-phase, multi-scale carbon nanotubes (CNTs), E-glass (alumino-borosilicate glass with less than 1% weight/weight alkali oxides) fibre reinforced polymer plates.

The focus of this thesis is to find the optimal graphene content along the thickness of the laminate, for different fibre types (glass or carbon) and distribution. Glass and carbon are common fibre types used in composites, the analysis will include these to present a realistic model. Additional design variables, such as the fibre content, stacking sequence and thickness ratio, are also used as these variables can be altered to assist in producing the optimum natural frequency when used in

conjunction with graphene. To investigate the aforementioned concept, a finite element analysis code is developed, using the first-order shear deformation theory (FSDT) [42], for the determination of the fundamental frequency of a multi-layered laminate. The code is then incorporated in an optimisation scheme, within sequential quadratic programming (SQP).

Section 2.2 of the thesis presents the theoretical background to the finite element analysis, developed to simulate the free vibration response of laminate plates. In Section 3 the micromechanical equations adopted in this study are given for the derivation of the effective material properties of the laminate. Section 4 presents the optimization formulation, and in Chapter 5, the verification of the proposed numerical scheme as well as the results of this study.

2.2 Theoretical formulation for the constituted behavior of a composite laminate and vibration within finite element analysis

A laminated composite plate having length *a*, width *b*, total thickness *h* is illustrated Figure 2.2.1. The plate consists of N number of uniformly thick layers with the principal material coordinates of the *k*th lamina oriented at an angle θ_k (fibre angle) to the laminate coordinate x. The *xy*−plane coincide with the midplane of the plate, with the z-axis being normal to the midplane. The kth layer is located between the points $z = z_k$ and $z = z_{k-1}$ in the thickness direction. Each layer of the plate is made of a polymer matrix reinforced with graphene nanoplatelets, wherein the volume fractions of graphene are different. An analysis of both constant graphene and differing graphene volume fractions is studied in this research to compare the resultant natural frequencies and determine a cost-effective composite laminate. In the graphene reinforced polymer matrix, fibre reinforcement is added as the traditional composite consist of a fibre as the reinforcement and graphene in this study will be the nano-reinforcement.

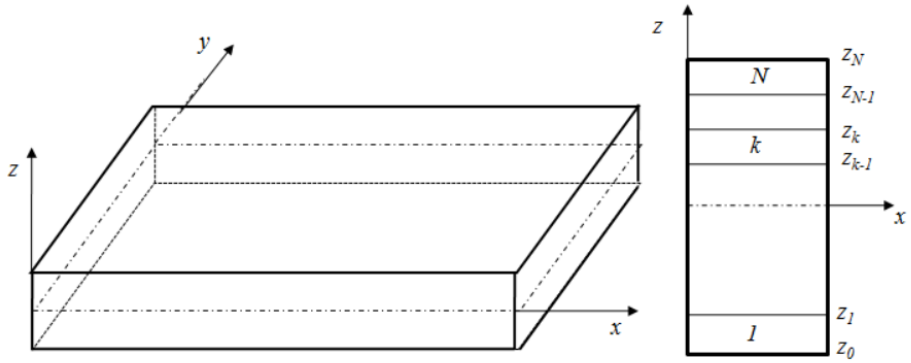

Figure 2.2. 1: Geometry of the laminated plate [42]

2.2.1 Mechanical displacements and strains

One of the most widely used displacement-based theories for laminated plates is the first-order shear deformation theory (FSDT) [42]. This theory is based on the displacement field from the following equations:

$$\begin{aligned} u_1\,(x,y,z,t) &= u(x,y,t) + z\varphi_x(x,y,t), \\ u_2\,(x,y,z,t) &= v(x,y,t) + z\varphi_y(x,y,t), \\ u_3\,(x,y,z,t) &= w(x,y,t) \end{aligned} \tag{1}$$

where, (u_1, u_2, u_3) are the displacements at any point of the plate along the (x, y, z) coordinates, (u, v, w) are the displacements associated with a point on the mid-plane of the panel, relative to the x, y and z-axis. φ_x and φ_y are the normal rotations, of a point on the midplane of the laminate in figure 2.2.1, about the x and y-axes, respectively.

The laminate plate will not be subject to damage, large deformation or permanent deformation after unloading therefore, we use the usual, liner elastic strain–displacement relations, the bending (ε_b) and shear strains (ε_s) can be written as

$$\{\varepsilon_b\} = \{\varepsilon_{0b}\} + z\{\kappa\}, \qquad \{\varepsilon_s\} = \{\varepsilon_{0s}\} \tag{2}$$

Where

$$\{\varepsilon_b\} = \{\varepsilon_{xx}, \varepsilon_{yy}, \gamma_{xy}\}^T, \{\varepsilon_s\} = \{\gamma_{yz}, \gamma_{xz}\}^T, \quad \{\varepsilon_{0b}\} = \left\{\frac{\partial_u}{\partial_x}, \frac{\partial_v}{\partial_y}, \frac{\partial_u}{\partial_y} + \frac{\partial_v}{\partial_x}\right\}^T \tag{3a}$$

$$\{\kappa\} = \left\{-\frac{\partial \varphi_x}{\partial x}, -\frac{\partial \varphi_y}{\partial y}, -\left(\frac{\partial \varphi_x}{\partial y} + \frac{\partial \varphi_y}{\partial x}\right)\right\}^T, \quad \{\varepsilon_{0s}\} = \left\{\frac{\partial w}{\partial y} - \varphi_y, \frac{\partial w}{\partial x} - \varphi_x\right\}^T \tag{3b}$$

2.2.2 Constitutive equations of the composite laminate

For a plate made of an orthotropic material (i.e. the plate possesses a plane of elastic symmetry parallel to the *x-y* plane), the linear constitutive equations for the *k*-th lamina in plane-stress state are given by:

$$\{\sigma\}_k = [Q]_k\{\varepsilon\} \tag{4}$$

where $\{\sigma\}$ is the stress tensor and $\{\varepsilon\}$ is the strain tensor. $[Q]$ is the *plane-stress reduced elastic stiffness* matrix. After separating the bending $\{\sigma_b\}$ and shear $\{\sigma_s\}$ related variables, the constitutive Eq. (4) becomes

$$\{\sigma_b\} = [Q_b]\{\varepsilon_b\}, \quad \{\sigma_s\} = [Q_s]\{\varepsilon_s\} \tag{5}$$

Where $\{\sigma_b\} = \{\sigma_1, \sigma_2, \sigma_6\}^T$, $\{\sigma_s\} = \{\sigma_4, \sigma_5\}^T$ and

$$[Q_b]_k = \begin{bmatrix} {Q_{11}}^{(k)} & {Q_{12}}^{(k)} & {Q_{16}}^{(k)} \\ {Q_{21}}^{(k)} & {Q_{22}}^{(k)} & {Q_{26}}^{(k)} \\ {Q_{61}}^{(k)} & {Q_{62}}^{(k)} & {Q_{66}}^{(k)} \end{bmatrix} \qquad [Q_s]_k = \begin{bmatrix} {Q_{44}}^{(k)} & {Q_{45}}^{(k)} \\ {Q_{54}}^{(k)} & {Q_{55}}^{(k)} \end{bmatrix} \tag{6}$$

Symmetry applies therefore: ${Q_{61}}^{(k)} = {Q_{16}}^{(k)} = 0$, ${Q_{12}}^{(k)} = {Q_{21}}^{(k)}$, ${Q_{26}}^{(k)} = {Q_{62}}^{(k)} = 0$ and ${Q_{54}}^{(k)} = {Q_{45}}^{(k)} = 0$

In Eq. (6), $Q_{ij}^{(k)}$ are the *plane stress reduced stiffnesses* of the *kth* lamina in its material coordinate system (x_1, x_2, x_3) given by [42]

$${Q_{11}}^{(k)} = \frac{{E_1}^{(k)}}{(1 - {v_{12}}^{(k)}{v_{21}}^{(k)})}, \qquad {Q_{12}}^{(k)} = \frac{{v_{12}}^{(k)}{E_2}^{(k)}}{(1 - {v_{12}}^{(k)}{v_{21}}^{(k)})}, \quad {Q_{22}}^{(k)} = \frac{{E_2}^{(k)}}{(1 - {v_{12}}^{(k)}{v_{21}}^{(k)})},$$

$${Q_{66}}^{(k)} = {G_{12}}^{(k)}, \qquad {Q_{44}}^{(k)} = {G_{23}}^{(k)}, \qquad {Q_{55}}^{(k)} = {G_{13}}^{(k)}$$

where $E_1^{(k)}$, $E_2^{(k)}$ are the effective longitudinal and transverse moduli of elasticity of the *k*-th layer, $v_{12}^{(k)}$, $v_{21}^{(k)}$ are the effective Poisson's ratios of the *k*-th layer and $G_{12}^{(k)}$, $G_{23}^{(k)}$, $G_{13}^{(k)}$ are the effective shear moduli of the *k*-th layer.

The reduced stiffness $Q_{ij}^{(k)}$ of the *k*-th lamina can be transformed to $\bar{Q}_{ij}^{(k)}$ in the coordinate system (x, y, z) as

$$\left[\overline{Q}\right]_{(k)} = ([T]^T[Q][T])_{(k)} \tag{7}$$

where $[T]$ is a transformation matrix considering the fibre angle *θ(k)* of the *k*th lamina [42].

2.2.3 Finite Element Formulation of the composite laminate

In this present study, the laminated plate model has been discretized using a four noded isoparametric quadrilateral Lagrangian element with five degrees of freedom (DOF) per node. This element is used since it can describe the structural response of the composite laminate [42]. The generalized displacement vector is interpolated as:

$$\{\overline{u}(x,y,t)\} \equiv \{u, v, w, \varphi_x, \varphi_y\}^T = [N_u]\{d\}_e = \sum_{j=1}^{4}\left(N_j[I]_{5x5}\{d_j\}_e\right) \tag{8}$$

where $\{d_j\}_e = \{u_j, v_j, w_j, \varphi_{xj}, \varphi_{yj}\}^T$ corresponding to the *j*-th node of the element and N_j is the shape functions.

Substituting (8) into Eq. (2) gives

$$\{\overline{\varepsilon}(x,y,t)\} = [B]\{d\}_e = \sum_{j=1}^{4}\left([B_j]\{d_j\}_e\right) \tag{9}$$

or equivalent

$$\{\overline{\varepsilon}\} = \begin{Bmatrix}\{\varepsilon_{b0}\}\\ \{\kappa\}\\ \{\varepsilon_{s0}\}\end{Bmatrix} = \begin{bmatrix}[B_b]\\ [B_k]\\ [B_s]\end{bmatrix}\{d\}_e = \sum_{j=1}^{4}\left(\begin{bmatrix}[B_b]_j\\ [B_k]_j\\ [B_s]_j\end{bmatrix}\{d_j\}_e\right) \tag{10}$$

where

$$[B_b]_j = \begin{bmatrix}\partial_x & 0 & 0 & 0 & 0\\ 0 & \partial_y & 0 & 0 & 0\\ \partial_y & \partial_x & 0 & 0 & 0\end{bmatrix}N_j, \quad [B_k]_j = \begin{bmatrix}0 & 0 & 0 & -\partial_x & 0\\ 0 & 0 & 0 & 0 & -\partial_y\\ 0 & 0 & 0 & -\partial_y & -\partial_x\end{bmatrix}N_j, \quad [B_s]_j = \begin{bmatrix}0 & 0 & \partial_x & -1 & 0\\ 0 & 0 & \partial_y & 0 & -1\end{bmatrix}N_j$$

and $\partial_x = \partial/\partial x$, $\partial_y = \partial/\partial y$.

2.2.4 Strain energy

The strain energy of the graphene reinforced composite plate element is expressed as

$$U = \frac{1}{2}\int_{V_e}\left(\{\varepsilon_{b0}\}^T\left[\overline{Q_b}\right]\{\varepsilon_{b0}\} + \{\varepsilon_{b0}\}^T z[\overline{Q_b}\{k\} + \{k\}^T z\left[\overline{Q_b}\right]\{\varepsilon_{b0}\} + \{k\}^T z^2\left[\overline{Q_b}\right]\{k\} + \{\varepsilon_{s0}\}^T[\overline{Q_s}]\{\varepsilon_{s0}\}\right)dV$$

$$= \frac{1}{2}\int_V \begin{Bmatrix}\{\varepsilon_{b0}\}\\ \{k\}\\ \{\varepsilon_{s0}\}\end{Bmatrix}^T \begin{bmatrix}[\overline{Q_b}] & z[\overline{Q_b}] & 0\\ z[\overline{Q_b}] & z^2[\overline{Q_b}] & 0\\ 0 & 0 & [\overline{Q_s}]\end{bmatrix}\begin{Bmatrix}\{\varepsilon_{b0}\}\\ \{k\}\\ \{\varepsilon_{s0}\}\end{Bmatrix} dV = \frac{1}{2}\int_V \{\overline{\varepsilon}\}^T[D(z)]\{\overline{\varepsilon}\}dV \quad (11)$$

where V is the volume of an element. Substituting for $\{\varepsilon_{b0}\}$, $\{\kappa\}$ and $\{\varepsilon_{s0}\}$ in the above equation, U can be written as

$$U = \frac{1}{2}\{d\}_e{}^T[K]_e\{d\}_e \quad (12)$$

where

$$[K]_e = \sum_{k=1}^{N}\left[\int_{V_k}[B\}^T[D(z)]_k[B]dV_k\right] \quad (13)$$

and V_k is the volume of the *k*-th layer and *N* is the number of lamina.

2.2.5 Kinetic energy

The kinetic energy of the graphene reinforced composite plate element is expressed as

$$T = \frac{1}{2}\sum_{k=1}^{N}\left(\int_{V_k}\rho_k\left[\{\dot{u_1}\}^2 + \{\dot{u_2}\}^2 + \{\dot{u_3}\}^2\right]dV_k\right), \quad (14)$$

where ρ_k is the density of the *k*-th layer. Substituting the displacements relations (1), Eq. (14) becomes

$$T = \frac{1}{2}\sum_{k=1}^{N}\left(\int_{V_k}\rho_k\left[\dot{u}^2 + 2z\dot{u}\varphi_x \dot{+} \dot{v}^2 + 2z\dot{v}\dot{\varphi}_y + \dot{w}^2 + z^2\dot{\varphi}^2 + z^2\dot{\varphi}_y^2\right]dV_k\right)$$

$$= \frac{1}{2}\sum_{k=1}^{N}\int_{V_k}\begin{Bmatrix} u \\ v \\ w \\ \varphi_x \\ \varphi_y \end{Bmatrix}^T \rho_k \begin{bmatrix} 1 & 0 & 0 & -z & 0 \\ 0 & 1 & 0 & 0 & -z \\ 0 & 0 & 1 & 0 & 0 \\ -z & 0 & 0 & z^2 & 0 \\ 0 & -z & 0 & 0 & z^2 \end{bmatrix}\begin{Bmatrix} u \\ v \\ w \\ \varphi_x \\ \varphi_y \end{Bmatrix} dV_k = \sum_{k=1}^{N}\frac{1}{2}\int_{V_k}\left\{\dot{\overline{u}}\right\}^T [I(z)]_k\{\dot{\overline{u}}\}dV_k \quad (15)$$

Substituting Eq. (8) in the above relation, one obtains

$$T = \frac{1}{2}\{\dot{d}\}^T[M]\{\dot{d}\} \quad (16)$$

where

$$[M]_e = \int_{A_e}\sum_{k=1}^{N}\int_{z_{k-1}}^{z_k}[N]^T[I(z)]_k[N]dzdA \quad (17)$$

where A_e is the area of the element. z_{k-1}, z_k are the *z* coordinates of laminates corresponding to the top and bottom surface of the *k*-th layer.

2.2.6 Work done by the mechanical forces

The work done by the mechanical forces is given by

$$W = \{\overline{u}\}^T\{f_c\} + \int_{S_1}\{\overline{u}\}^T\left\{f_s^{(i)}\right\}dS + \int_V\{\overline{u}\}^T\{f_v\}dV$$

$$= \{d\}_e{}^T[N]^T\{f_c\} + \{d\}_e{}^T\int_{S_1}[N]^T\left\{f_s^{(i)}\right\}dS + \{d\}_e{}^T\int_V[N]^T\{f_v\}dV \equiv \{d\}_e{}^T\{F_m\}_e \quad (18)$$

In Eq. (18), the concentrated force vector is denoted by the symbol $\{f_c\}$ and the surface and volume force vectors are denoted by the symbols, $\{f_s\}$ and $\{f_v\}$ respectively. S_1 is the surface area where the mechanical forces are applied. $\{F_m\}_e$ is the applied mechanical forces in an element.

2.2.7 Governing equation of the eigenvalue problem for the composite laminate

Using Hamilton's principle, the governing equation of the graphene reinforced composite plate subjected to mechanical loading is expressed as

$$\int_0^T (\delta T - \delta U + \delta W)\, dt = 0 \tag{19}$$

Substituting the values of *U*, *T* and *W*, the global form of the final governing equation is expressed as

$$[M]\{\ddot{d}\} + [K]\{d\} = \{F_m\} \tag{20}$$

where [*M*], [*K*], {*d*} and {F_m} are global mass matrix, global linear stiffness matrix, global displacement and force vector, respectively.

The generalized governing equation (20) can be employed to study the free vibration by dropping the force term as:

$$[K]\{d\} = \lambda[M]\{d\} \tag{21}$$

with $\lambda = \omega^2$, where ω is defined as frequency of natural vibration.

2.3. Effective material properties using micromechanics equations

The nanocomposite laminate which is studied in this thesis, consists of a 3-phase graphene/fibre reinforced polymer matrix. Two phases of micromechanical equations are adopted to provide the effective material properties of the overall multi-scale laminate. The effective material properties are the average material properties of the materials involved in the composite so that each material has been taken into account [42]. In phase 1, the effective material properties of the graphene reinforced matrix are calculated. Within this micromechanical law, GPLs are considered to be

uniformly distributed in the polymer matrix. In phase 2, the effective material properties of the overall graphene/fibre reinforced composite are obtained.

2.3.1 Graphene Reinforced Matrix

In this section, the effective Young's modulus, Poisson's ratio, Shear modulus and density are derived for the graphene reinforced matrix, using micromechanical equations presented in [43, 44, 45, 46]. In the equations below, the subscripts GPL, M and GM are used for the graphene nanoplatelets (GPL), the matrix (M) and the effective graphene reinforced matrix (GM).The effective Young's module for the graphene reinforced matrix is given in Eq. (22).

$$E_{GM} = \left(\frac{3}{8}\frac{1+\xi_{\mathrm{L}}\eta_L V_{GPL}}{1-\eta_L V_{GPL}} + \frac{5}{8}\frac{1+\xi_w\eta_w V_{GPL}}{1-\eta_w V_{GPL}}\right) \times \mathrm{E_M} \tag{22}$$

The volume content of the graphene platelets is represented in Eq. (22) as $V_{GPL.}$ Parameters ξ_{L} and ξ_w are derived in Eq. (23) using the platelets' dimensions, namely, the length (l_{GPL}), the width (w_{GPL}) and the thickness (h_{GPL}).

$$\xi_{\mathrm{L}} = 2\frac{l_{GPL}}{h_{GPL}}, \quad \xi_w = 2\frac{w_{GPL}}{h_{GPL}} \tag{23}$$

Symbols η_L and η_w used in Eq. (22) are calculated below, using Young's moduli of the graphene nanoplatelets E_{GPL} and the matrix E_M

$$\eta_L = \frac{(E_{GPL}/E_M)-1}{(E_{GPL}/E_M)+\xi_{\mathrm{L}}}, \qquad \eta_w = \frac{(E_{GPL}/E_M)-1}{(E_{GPL}/E_M)+\xi_w} \tag{24}$$

The content of graphene nanoplatelets may also be provided in terms of its weight fraction W_{GPL}, indicating that the volume fraction can be computed from

$$V_{GPL} = \frac{W_{GPL}}{W_{GPL}+(\rho_{GPL}/\rho_M)(1-W_{GPL})} \tag{25}$$

where ρ_{GPL} and ρ_M represent the mass density of graphene nanoplatelets and the polymer matrix, respectively. Poisson's ratio, the Shear modulus and the density for the graphene reinforced matrix are given by

$$v_{GM} = v_{GPL}V_{GPL} + v_M(1-V_{GPL}) \tag{26}$$

$$G_{GM} = \frac{E_{GM}}{2(1+v_{GM})} \quad (27)$$

$$\rho_{GM} = \rho_{GPL} V_{GPL} + \rho_M (1 - V_{GPL}) \quad (28)$$

2.3.2 Fibre Reinforcement of the graphene/polymer matrix

Fibres, which are traditional reinforcement in composites, further improve the overall material properties of the graphene reinforced polymer matrix by providing strength to the composite. Unidirectional continuous fibres are considered, inducing directional strength and stiffness. The effective Young's moduli, Shear modulus, Poisson's ratio and density of the fibre/graphene reinforced nanocomposite, respectively, are computed via the micromechanical relations given in [47].

$$E_{11} = E_{F11} V_F + E_{GM} (1 - V_F) \quad (29)$$

$$E_{22} = E_{GM} \left(\frac{E_{F22} + E_{GM} + (E_{F22} - E_{GM}) V_F}{E_{F22} + E_{GM} - (E_{F22} - E_{GM}) V_F} \right) \quad (30)$$

$$G_{12} = G_{GM} \left(\frac{G_{F12} + G_{GM} + (G_{F12} - G_{GM}) V_F}{G_{F12} + G_{GM} - (G_{F12} - G_{GM}) V_F} \right) \quad (31)$$

$$v_{12} = v_{F12} V_F + v_{GM} (1 - V_F) \quad (32)$$

$$\rho = \rho_F V_F + \rho_{GM} (1 - V_F) \quad (33)$$

Subscripts GM and F refer to graphene reinforced matrix and fibres, respectively. The fibre volume content is represented by V_F and the fibre density by ρ_F.

2.4. Optimization framework for maximizing the fundamental frequency of the composite laminate

The adopted optimization scheme is presented in this section. The goal is to maximize the fundamental frequency of the laminate plate in order to decrease the possibility of encountering resonance, considering several parameters, such as the weight of graphene, fibre angle, stacking sequence, thickness, aspect ratio and fibre content. The general optimization scheme is presented in Eq. (34):

$$\max Natural\ Frequency\ f(V_F, W_{GPL}, \theta) = \Omega \quad (34)$$

$$subject\ to\ \sum_{k=1}^{n} W_{GPL} = b \quad (34b)$$

$$c_1 \leq W_{GPL} \leq c_2 \quad (34c)$$

$$d_1 \leq V_F \leq d_2 \quad (34d)$$

$$-90^o \leq Fibre\ angle\ \theta \leq 90^o \quad (34e)$$

$$\sum_{k=1}^{n} \frac{h_k}{D} = 1 \quad (34f)$$

Eq. (34b) states that the summation of the graphene weight (W_{GPL}) per layer for the total number of layers (*n*), thus, the total graphene weight for the laminate, is set to a predetermined number (both 10% and 20% of graphene by weight has been tested in this thesis). Eq. (34c) and (34d) describe that a lower and an upper limit for graphene weight and fibre content (V_F) per layer have been set. When a non-uniform thickness per layer is considered, the thickness of each layer becomes another variable of the problem, Eq. (34f) is then adopted. In Eq. (34f), the thickness ratio h_k/D is defined as the thickness of each layer over the total thickness of the laminate. For the solution of the optimisation problem, a Sequential Quadratic Programming algorithm (SQP) is adopted. This is an effective method which generates steps by solving quadratic subproblems, for nonlinearly constrained optimization [48]. In particular, an approximation of the Hessian of the Lagrangian function is considered at each major iteration, using a quasi-Newton updating method. This is then used to generate a Quadratic Programming subproblem whose solution is used to define a search direction. This scheme is briefly presented below.

The optimization problem with nonlinear equality and inequality constraints is given by [48]:

$$\begin{gathered} \min f(x) \\ subject\ to\ c_i(x) = 0, i \in E \\ c_i(x) \geq 0, i \in I \end{gathered} \tag{35}$$

The problem is then linearized into:

$$\begin{gathered} \min_p f_k + \nabla f_k^T p + \frac{1}{2} p^T \nabla_{xx}^2 L_k p \\ subject\ to\ \nabla c_i(x_k)^T p + c_i(x_k) = 0, i \in E \\ \nabla c_i(x_k)^T p + c_i(x_k) \geq 0, i \in I \end{gathered} \tag{36}$$

The solution of the presented problem is implemented within MATLAB [49, 50]. It is noted that since the mentioned MATLAB algorithms are originally defined for minimization, the objective function presented in Eq. (34) is modified as follows: $\min Natural\ Frequency\ f(V_F, W_{GPL}, \theta) = -\Omega$.

CHAPTER 3: Results and Discussions

3.1 Verification of the proposed approach

In the numerical results section, the non-dimensional form Ω of the fundamental frequency ω is used which is given by

$$\Omega = \omega D \sqrt{\frac{\rho_M}{E_M}} \quad [51]$$

To verify the results obtained from the method which is presented in this work, comparisons with published research and commercial software have been considered. The commercial software is widely used and accepted by the scientific community. In several papers published in recognized international journals, comparison of the results provided by commercial software and the results derived by a numerical code (Matlab in this thesis), is used to verify the code [34]. For the subsequent simulations, related to the optimization for the composite laminate in this section, the material properties shown in Table 3.1.1 and the geometry of GPLs: $Length_{GPL}$ = 2.5 μm, $Width_{GPL}$ = 1.5 μm, $Thickness_{GPL}$ = 1.5nm are used. The graphene weight is considered equal to W_{GPL} = 1%.

First, a comparison of the natural frequencies obtained by the proposed model is presented in Table 3.1.2. The proposed model utilizes GPL reinforced composite laminate's frequencies found in published literature. Comparison takes place for the case of an isotropic plate (zero graphene and fibre content), as well as for the case of GPL reinforced composite (zero fibre content). As shown in Table 3.1.2, for both cases, a comparison between published research and the model results in a good agreement.

The boundary conditions considered in this research are four different boundary conditions: Simply Supported (SSSS); Clamped (CCCC); Clamped on one edge and free on three edges (cantilever, CFFF) as well as simply supported and Clamped in opposite edges (SCSC).

Table 3.1. 1: Material properties of GPLs, matrix, carbon and glass fibres

Material	**E_{11}(GPa)**	**E_{22} (GPa)**	**G_{12} (GPa)**	υ_{12}	**Density (kg/m^3)**
GPL	1010	1010	E/(2(1+v))	0.186	1060
Matrix (ρ_M)	3	3	E/(2(1+v))	0.34	1200
Carbon fibres	263	19	27.60	0.20	1750
Glass fibres	72.4	72.4	E/(2(1+v))	0.20	2400

Table 3.1. 2: Comparison of natural frequencies Ω of GPLs reinforced square plates

Pattern	**Method**	**Non-dimensionalized Natural Frequencies**			
		Mode 1	**Mode 2**	**Mode 3**	**Mode 4**
Isotropic plate	Present/Mesh 5x5	0.0610	0.1611	0.1611	0.1951
	Present/Mesh 10x10	0.0590	0.1441	0.1441	0.1927
	Present/Mesh 15x15	0.0587	0.1413	0.1413	0.1923
	Ref. [26]	0.0584	0.1391	-	0.2132
	Ref. [52]	0.0584	0.1390	0.1919	0.2127
Uniformly distributed GPLs (1%) per laminate's thickness	Present/Mesh 5x5	0.1267	0.3352	0.3352	0.4064
	Present/Mesh 10x10	0.1228	0.2999	0.2999	0.4014
	Present/Mesh 15x15	0.1221	0.2941	0.2941	0.4005
	Ref. [26]	0.1216	0.2895	-	0.4436
	Ref. [52]	0.1216	0.2895	0.3999	0.4434

Note: The above consists of Simply Supported (SSSS) square plates with [D (total thickness) / L (Length)] = 0.1

The same composite laminate has been developed in ABAQUS commercial finite element analysis package. A comparison between the proposed models is also presented. Four node shell elements and a 10x10 mesh have been used in ABAQUS. As shown in Table 3.1.3, several cases have been examined, with one or more layers, different fibre angles, different boundary conditions. For all these cases, glass fibres are used with a fibre content equal to 50% for every layer. Results indicate a good agreement between the natural frequencies obtained by the model developed in this research and the commercial software.

Table 3.1. 3: Comparison of non-dimensionalized frequencies Ω of GPLs/glass fibre square plate

				Non-dimensionalized Natural Frequencies			
Boundary conditions	**Pattern**	**Stacking sequence of fibre angle (°)**	**Method**	**Mode**			
				1	**2**	**3**	**4**
SSSS	1 layer	45	Present	0.1579	0.3647	0.3870	0.5624
			Commercial software	0.1555	0.3601	0.3818	0.5568
	3 layers	0/90/0	Present	0.1500	0.3498	0.3945	0.4784
			Commercial software	0.1483	0.3454	0.3898	0.4806
	8 layers	0/30/45/90/ 90/45/30/0	Present	0.1530	0.3565	0.3916	0.5187
			Commercial software	0.1511	0.3520	0.3873	0.5173
CCCC	8 layers	0/30/45/90/ 90/45/30/0	Present	0.2639	0.4937	0.5325	0.7087
			Commercial software	0.2611	0.4885	0.5294	0.7018
SCSC	8 layers	0/30/45/90/ 90/45/30/0	Present	0.2226	0.3891	0.5137	0.5188
			Commercial software	0.2204	0.3844	0.5112	0.5190

Note : thickness/length ratio [D / L] = 0.1, W_{GPL} = 1% and fibre content equal to 50%.

The fibre angles in Table 3.1.3 as well as in all the examples presented later in the thesis are the angular orientation of the fibres measured in degrees and are relative to the x-axis.

To complete the validation of the proposed model, the optimal fundamental frequency which is obtained by the proposed approach, is compared with a number of discrete simulations conducted in commercial software ABAQUS. A two-layer hybrid laminate is chosen with a varying fibre angle per layer. Several simulations are then considered within the commercial software, with different combinations of fibre angles. As shown in Table 3.1.4, both the proposed approach and the commercial software result in the same optimal pair of fibre angles and a very close value for the optimal fundamental frequency.

Table 3.1. 4: Comparison of Ω with those obtained from commercial software

Commercial software discrete simulations			Proposed optimization code	
Case	Fibre angle per layer in Degrees (°)	Non-dimensionalized frequency (Ω)	Optimal Fibre angle in Degrees (°)	Optimal non-dimensionalized frequency
1	0/0	0.1483	**45/45**	**0.1579**
2	30/0	0.1505		
3	45/0	0.1510		
4	60/0	0.1496		
5	90/0	0.1464		
6	0/30	0.1505		
7	30/30	0.1537		
8	45/30	0.1543		
9	60/30	0.1528		
10	90/30	0.1496		
11	0/45	0.1510		
12	30/45	0.1543		
13	**45/45**	**0.1555**		
14	60/45	0.1543		
15	90/45	0.1510		
16	0/60	0.1496		
17	30/60	0.1528		
18	45/60	0.1543		
19	60/60	0.1537		
20	90/60	0.1505		
21	0/90	0.1464		
22	30/90	0.1496		
23	45/90	0.1510		
24	60/90	0.1505		
25	90/90	0.1483		

The results in Table 3.1.4 are for a GPLs/Glass fibre SSSS square plate with [D / L] = 0.1, WGPL=1% and fibre content equal to 50%).

3.1.1 Analysis of the effects of reinforcements on frequencies for the composite laminate

Before presenting the results for the optimal design question, some preliminary simulations are conducted with the GPLs and fibres distributed uniformly across the layers, i.e., all layers having the same volume content of the reinforcements. The objective of this study is to assess the effect of different graphene and/or fibre contents on the fundamental frequency (Ω) and to study the trends as reinforcements increase. This study is conducted to observe the behaviour of 3-phase composites which may have some unusual trends in terms of the effect of different reinforcements on frequencies.

For this purpose, uniform glass or carbon fibre contents of 30% or 60% are specified for each layer, in an 8-layered laminate. The results of this exercise are shown in Figs. 3.1.1.1 to 3.1.1.4 for different boundary conditions. In Fig. 3.1.1.1 and 3.1.1.2 results for an anti-symmetric stacking sequence are given. In Fig. 3.1.1.3 and 3.1.1.4 a symmetric stacking sequence is given.

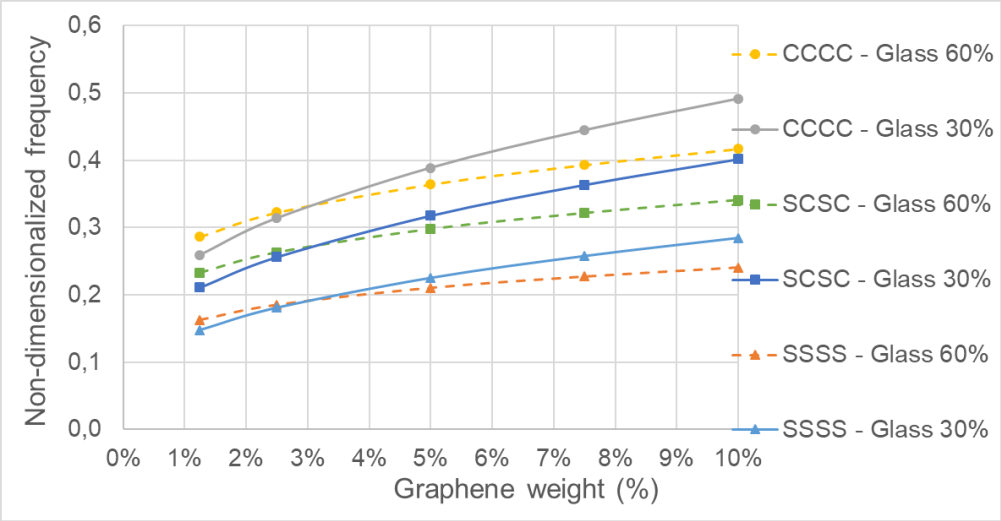

Figure 3.1.1. 1: Shows Ω with uniform graphene and fibre distributions in all layers with anti-symmetric stacking sequence $[0/90/0/90]_{anti\text{-}sym}$, D/L = 0.1 , a/b =1, for glass fibres

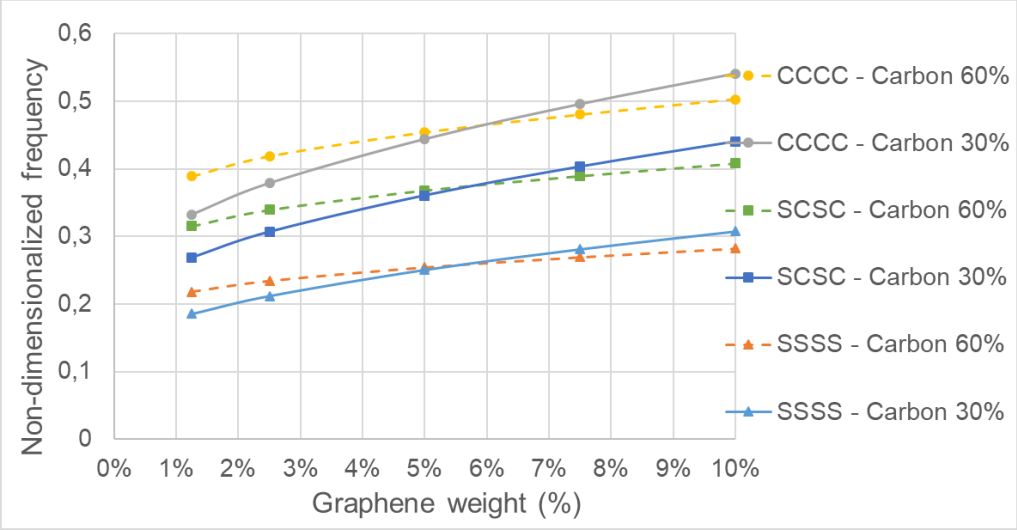

Figure 3.1.1. 2: Shows Ω with uniform graphene and fibre distributions in all layers with anti-symmetric stacking sequence $[0/90/0/90]_{anti\text{-}sym}$, D/L = 0.1 , a/b =1, for carbon fibres

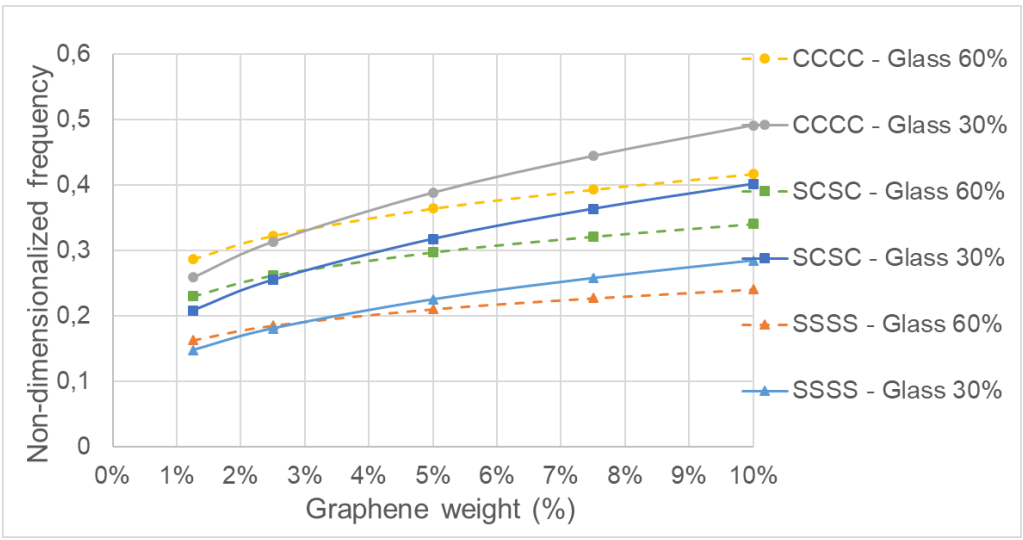

Figure 3.1.1. 3: Ω with uniform graphene and fibre distributions in all layers, symmetric stacking sequence $[90/0/90/0]_{sym}$, D/L = 0.1 , a /b = 1, for glass fibres

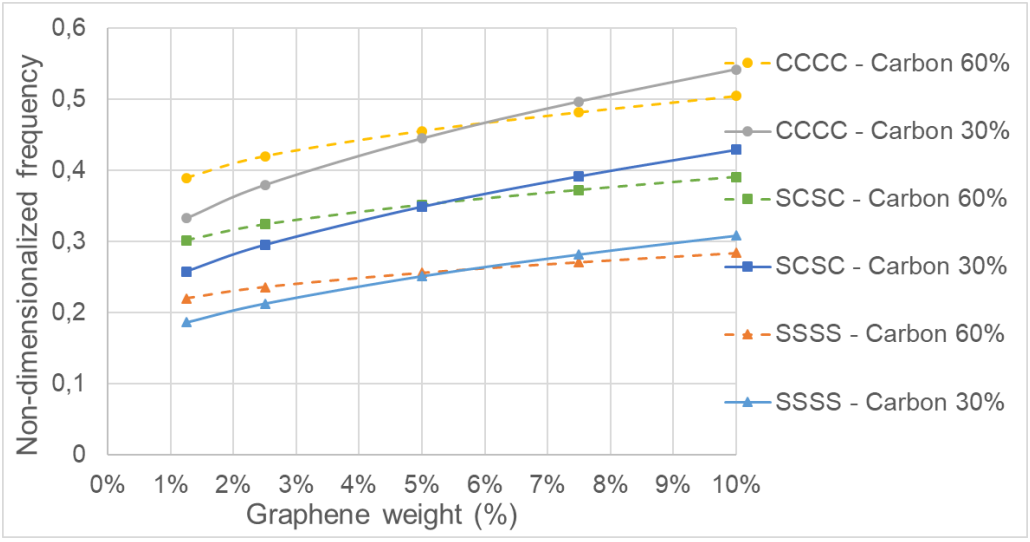

Figure 3.1.1. 4: Ω with uniform graphene and fibre distributions in all layers, symmetric stacking sequence $[90/0/90/0]_{sym}$, D/L = 0.1 , a /b = 1, for carbon fibres

It can be observed from Figs. 3.1.1.1 to 3.1.1.4 that as the graphene weight increases beyond a certain limit, a lower percentage of fibres (30%) results in a higher frequency as compared to the higher percentage of fibres (60%) for both glass and carbon fibres. This cross-over point for glass fibres is approximately 3% of graphene weight and for carbon fibres approximately 6% of graphene weight. This observation indicates that the optimal distribution of graphene and the fibres along the thickness of the laminate needs to be taken into account for an efficient design since a simplified consideration, e.g., of the uniform distribution of graphene reinforcement across the thickness may lead to diminishing returns or inefficient design.

The results indicate that higher fibre content does not lead to higher frequencies at increased graphene content since increasing the fibre content has the effect of reducing the frequency if the graphene content exceeds a certain threshold. It is observed that this threshold value is higher for carbon fibre reinforced laminates as compared to glass fibre reinforced laminates. This effect is due to the higher stiffness of the carbon fibres.

The effect of the high stiffness of the graphene takes place at higher graphene contents if the fibres have high stiffness (carbon fibre) and this effect happens earlier if the fibres have low stiffness (glass fibre). It is observed that the two different

stacking sequences shown in Figs. 3.1.1.1 to 3.1.1.4 namely, cross-ply anti-symmetric and symmetric, result in similar behaviours.

3.2 Results of the optimization analysis for maximizing the fundamental frequency of the composite laminate

The optimization problem of the graphene/fibre reinforced nanocomposite plate is studied in this section. In the simulations several design variables for four different boundary conditions are numerically tested: Simply Supported (SSSS); Clamped (CCCC); clamped on one edge and free on three edges (cantilever), (CFFF) as well as simply supported and clamped in opposite edges (SCSC). The simulations are conducted for an eight-layer laminate nanocomposite plate, with the design variables of the graphene weight, the fibre content, the fibre angle, the thickness ratio. The thickness ratio is defined as the thickness of each layer over the total thickness of the laminate (h/D). The ratio of the total thickness of the laminate over the length of one edge (D/L), as well as the aspect ratio (L_y/L_x) as the ratio between the length of the two edges are defined. A stacking sequence given in the captions of the tables is randomly selected for the first simulations. Then, different stacking sequences are considered.

3.2.1 Influence of graphene weight on natural vibration (optimization problem with one design variable)

In the initial test, graphene weight (W_{GPL}) is the design variable of the problem, which is limited between 0.01 and 0.1 (1% - 10%) per layer. For all tests, an 8-layer laminate is considered. A uniform fibre content of 30% or 60% is assigned for every layer of the laminate for both glass and carbon fibre. The optimum frequencies (maximum fundamental frequency for the laminate under consideration) and the corresponding design variables for this case are presented in Table 3.2.1.1, for the four boundary conditions (BCs):

Table 3.2.1. 1: Optimum fundamental natural frequencies (Ω) with one variable: 1% ≤ WGPL ≤10% per layer

BCs		Optimal W_{GPL}	Ω
SSSS	**Glass 30%**	[0.1 / 0.1 / 0.1 / 0.1 / 0.1 / 0.1 / 0.1 / 0.1]	0.2845
	Glass 60%	[0.1 / 0.1 / 0.1 / 0.1 / 0.1 / 0.1 / 0.1 / 0.1]	0.2410
	Carbon 30%	[0.1 / 0.1 / 0.1 / 0.1 / 0.1 / 0.1 / 0.1 / 0.1]	0.3080
	Carbon 60%	[0.1 / 0.1 / 0.1 / 0.1 / 0.1 / 0.1 / 0.1 / 0.1]	0.2820
CCCC	**Glass 30%**	[0.1 / 0.1 / 0.1 / 0.1 / 0.1 / 0.1 / 0.1 / 0.1]	0.4916
	Glass 60%	[0.1 / 0.1 / 0.1 / 0.1 / 0.1 / 0.1 / 0.1 / 0.1]	0.4171
	Carbon 30%	[0.1 / 0.1 / 0.1 / 0.1 / 0.1 / 0.1 / 0.1 / 0.1]	0.5410
	Carbon 60%	[0.1 / 0.1 / 0.1 / 0.1 / 0.1 / 0.1 / 0.1 / 0.1]	0.5030
CFFF	**Glass 30%**	[0.1 / 0.1 / 0.1 / 0.1 / 0.1 / 0.1 / 0.1 / 0.1]	0.0509
	Glass 60%	[0.1 / 0.1 / 0.1 / 0.1 / 0.1 / 0.1 / 0.1 / 0.1]	0.0432
	Carbon 30%	[0.1 / 0.1 / 0.1 / 0.1 / 0.1 / 0.1 / 0.1 / 0.1]	0.0591
	Carbon 60%	[0.1 / 0.1 / 0.1 / 0.1 / 0.1 / 0.1 / 0.1 / 0.1]	0.0576
SCSC	**Glass 30%**	[0.1 / 0.1 / 0.1 / 0.1 / 0.1 / 0.1 / 0.1 / 0.1]	0.5697
	Glass 60%	[0.1 / 0.1 / 0.1 / 0.1 / 0.1 / 0.1 / 0.1 / 0.1]	0.4885
	Carbon 30%	[0.1 / 0.1 / 0.1 / 0.1 / 0.1 / 0.1 / 0.1 / 0.1]	0.6245
	Carbon 60%	[0.1 / 0.1 / 0.1 / 0.1 / 0.1 / 0.1 / 0.1 / 0.1]	0.5777

Note: D/L = 0.1, aspect ratio = 1 and fibre stacking sequence [0/90/0/90/0/90/0/90]:

The resultant optimal graphene weight required the maximum values (0.1), as determined by the analysis, for each fibre type and fibre content, as shown in Table 3.2.1.1. The graphene weight is optimal as this weight produced the highest fundamental frequency. In addition, a lower percentage of fibres (30%) results in a higher fundamental frequency for both glass and carbon fibers. The trend, for an increase from 30% to 60% fibres, is a 14%-15% decrease in fundamental frequency for glass and a decrease of 7%-8% for carbon fibre. Due to the properties such as Young's modulus and shear modulus for carbon being higher than glass, there is a smaller decrease in the fundamental frequency for carbon than glass fibres.

The CFFF boundary condition for carbon fibre shows a 2.5% decrease from 30%-60% fibres. All the simulations highlight that carbon fibres produce higher optimal fundamental frequency than glass fibres which is expected, due to the higher

material properties of carbon fibres. The largest optimal frequencies are observed for the SCSC boundary conditions, 0.5697 for glass and 0.6245 for carbon fibre. Figure 3.2.1.1 shows a graphical representation of the results in Table 3.2.1.1.

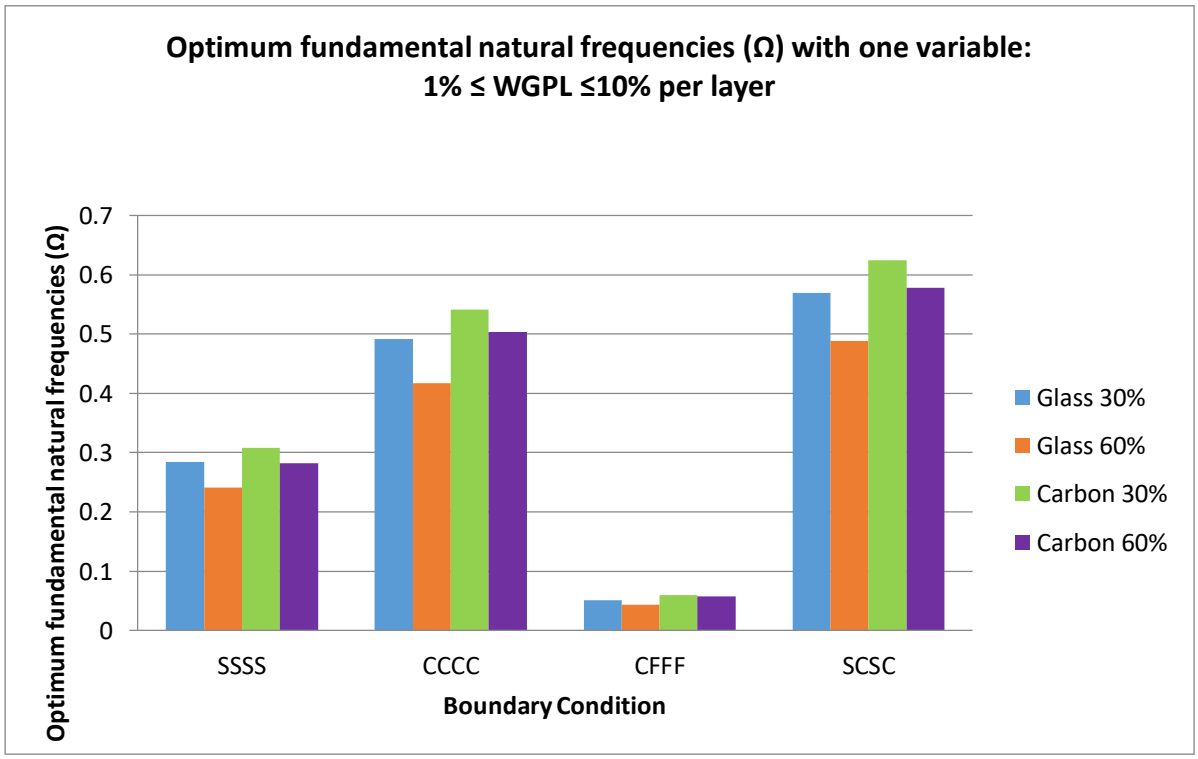

Figure 3.2.1. 1: Graphical representation of result from Table 3.2.1.1

This figure clearly shows that when the fibre content increases from 30% to 60%, the fundamental frequency decreases.

Figure 3.2.1.2 to 3.2.1.5 shows the eigenmodes (natural frequencies) for each boundary condition relating to the results of table 3.2.1.1. These figures were a product of the Matlab analysis.

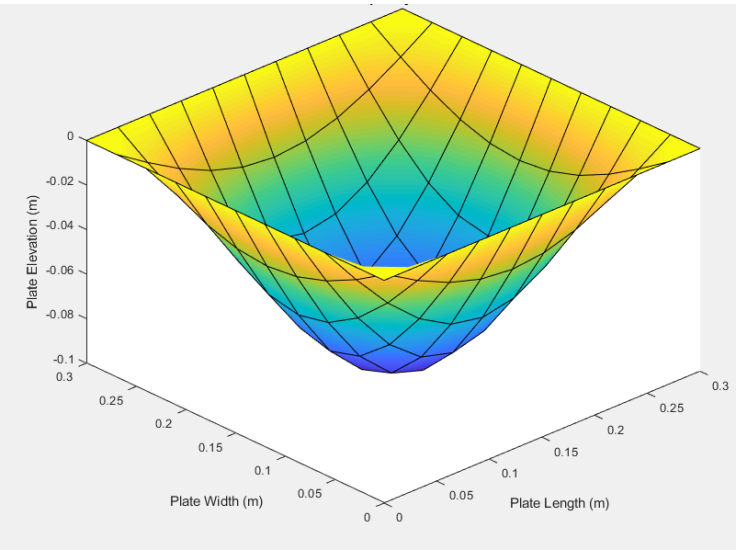

Figure 3.2.1. 2: Showing the first eigenmode for SSSS with 30% Glass

Figure 3.2.1.2 shows the first eigenmode for the analysis of the SSSS boundary condition for 30% glass fibres. This simulation produced a fundamental frequency of 0.2845.

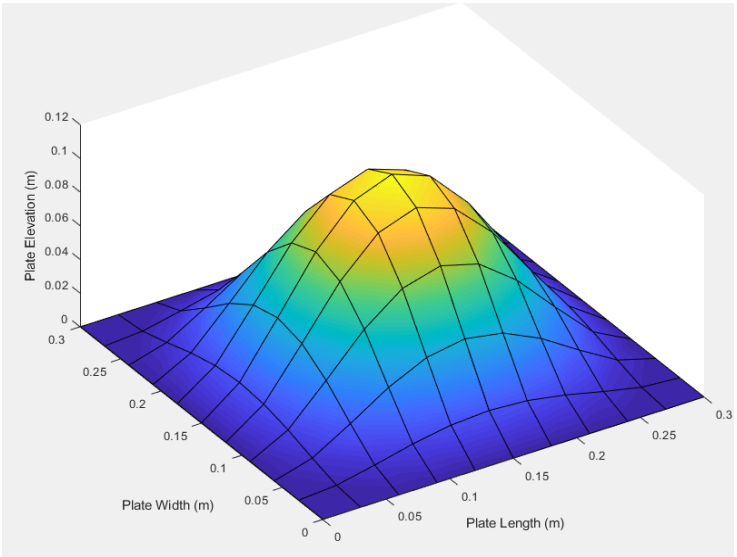

Figure 3.2.1. 3: Showing the first eigenmode for CCCC with 30% Glass

Figure 3.2.1.3 shows the first eigenmode for the CCCC boundary condition with 30% glass fibres resulting in a fundamental frequency of 0.4916.

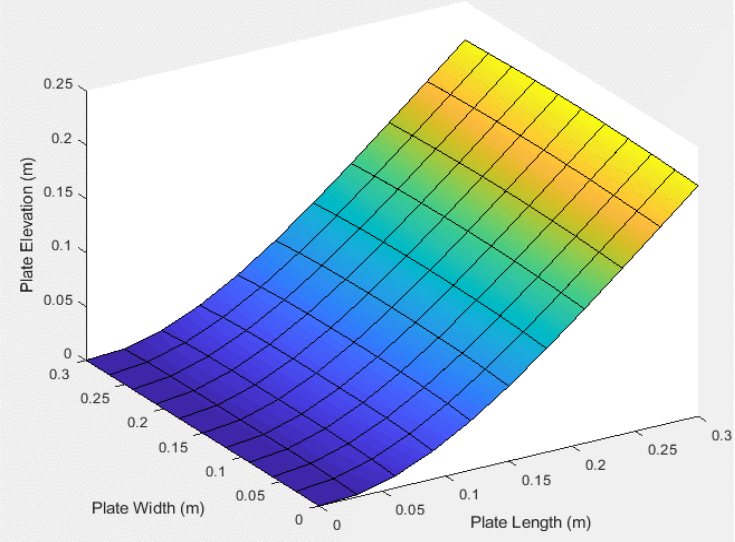

Figure 3.2.1. 4: Showing the first eigenmode for CFFF with 30% Glass

Figure 3.2.1.4 shows the first eigenmode for the CFFF boundary condition with 30% glass fibres resulting in a fundamental frequency of 0.0509.

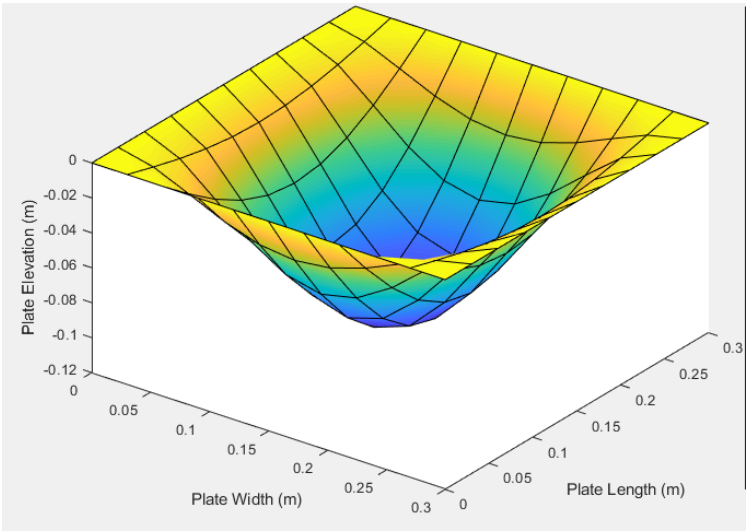

Figure 3.2.1. 5: Showing the first eigenmode for SCSC with 30% Glass

Figure 3.2.1.3 shows the first eigenmode for the SCSC boundary condition with 30% glass fibres resulting in a fundamental frequency of 0.5697.

To investigate the influence of the upper limit of the design variable (graphene weight), a new, reduced upper limit equal to 2.5% (instead of 10%) per layer is tested and results are given in Table 3.2.1.2.

Table 3.2.1. 2: Optimum fundamental natural frequencies (Ω) with one variable: 1% ≤ WGPL ≤2.5% per layer

BCs		Optimal W_{GPL}	Ω
SSSS	**Glass 30%**	[0.025 / 0.025 / 0.025 / 0.025 / 0.025 / 0.025 / 0.025 / 0.025]	0.181
	Glass 60%	[0.025 / 0.025 / 0.025 / 0.025 / 0.025 / 0.025 / 0.025 / 0.025]	0.185
	Carbon 30%	[0.025 / 0.025 / 0.025 / 0.025 / 0.025 / 0.025 / 0.025 / 0.025]	0.212
	Carbon 60%	[0.025 / 0.025 / 0.025 / 0.025 / 0.025 / 0.025 / 0.025 / 0.025]	0.234
CCCC	**Glass 30%**	[0.025 / 0.025 / 0.025 / 0.025 / 0.025 / 0.025 / 0.025 / 0.025]	0.314
	Glass 60%	[0.025 / 0.025 / 0.025 / 0.025 / 0.025 / 0.025 / 0.025 / 0.025]	0.323
	Carbon 30%	[0.025 / 0.025 / 0.025 / 0.025 / 0.025 / 0.025 / 0.025 / 0.025]	0.379
	Carbon 60%	[0.025 / 0.025 / 0.025 / 0.025 / 0.025 / 0.025 / 0.025 / 0.025]	0.419
CFFF	**Glass 30%**	[0.025 / 0.025 / 0.025 / 0.025 / 0.025 / 0.025 / 0.025 / 0.025]	0.033
	Glass 60%	[0.025 / 0.025 / 0.025 / 0.025 / 0.025 / 0.025 / 0.025 / 0.025]	0.034
	Carbon 30%	[0.025 / 0.025 / 0.025 / 0.025 / 0.025 / 0.025 / 0.025 / 0.025]	0.044
	Carbon 60%	[0.025 / 0.025 / 0.025 / 0.025 / 0.025 / 0.025 / 0.025 / 0.025]	0.051
SCSC	**Glass 30%**	[0.025 / 0.025 / 0.025 / 0.025 / 0.025 / 0.025 / 0.025 / 0.025]	0.256
	Glass 60%	[0.025 / 0.025 / 0.025 / 0.025 / 0.025 / 0.025 / 0.025 / 0.025]	0.263
	Carbon 30%	[0.025 / 0.025 / 0.025 / 0.025 / 0.025 / 0.025 / 0.025 / 0.025]	0.307
	Carbon 60%	[0.025 / 0.025 / 0.025 / 0.025 / 0.025 / 0.025 / 0.025 / 0.025]	0.339

Note: D/L = 0.1, aspect ratio = 1 and fibre stacking sequence [0/90/0/90/0/90/0/90]:

Contrary to the results presented in Table 3.2.1.1, when the limit for the maximum graphene weight per layer is 2.5% instead of 10% as given in Table 3.2.1.2, then an increase in the fibre content from 30% to 60% increases the natural frequency. The natural frequency in Table 3.2.1.2 across four boundary conditions, with an increase from 30% to 60% fibres, for glass resulted in an increase of 2.1% to 2.94%. For Carbon the increase in fibres increased the natural frequency by a range of 9.4% to 13.73%. In both cases (3.2.1.1 and 3.2.1.2), the graphene weight corresponding to the optimum natural frequency, which is the maximum natural frequency of the laminate, is the maximum permitted per layer (10% and 2.5%, respectively). In addition, the maximum optimal frequencies are obtained for the CCCC and not from the SCSC boundary conditions which was the case in Table 3.2.1.1. Comparison between Table 3.2.1.1 and 3.2.1.2 also shows that when the graphene limit per layer

was decreased, the fundamental frequency was decreased. This result is not true for CFFF as a decrease in W_{GPL} per layer increased the fundamental frequency. Figure 3.2.1.6 illustrates the results from Table 3.2.1.2 graphically.

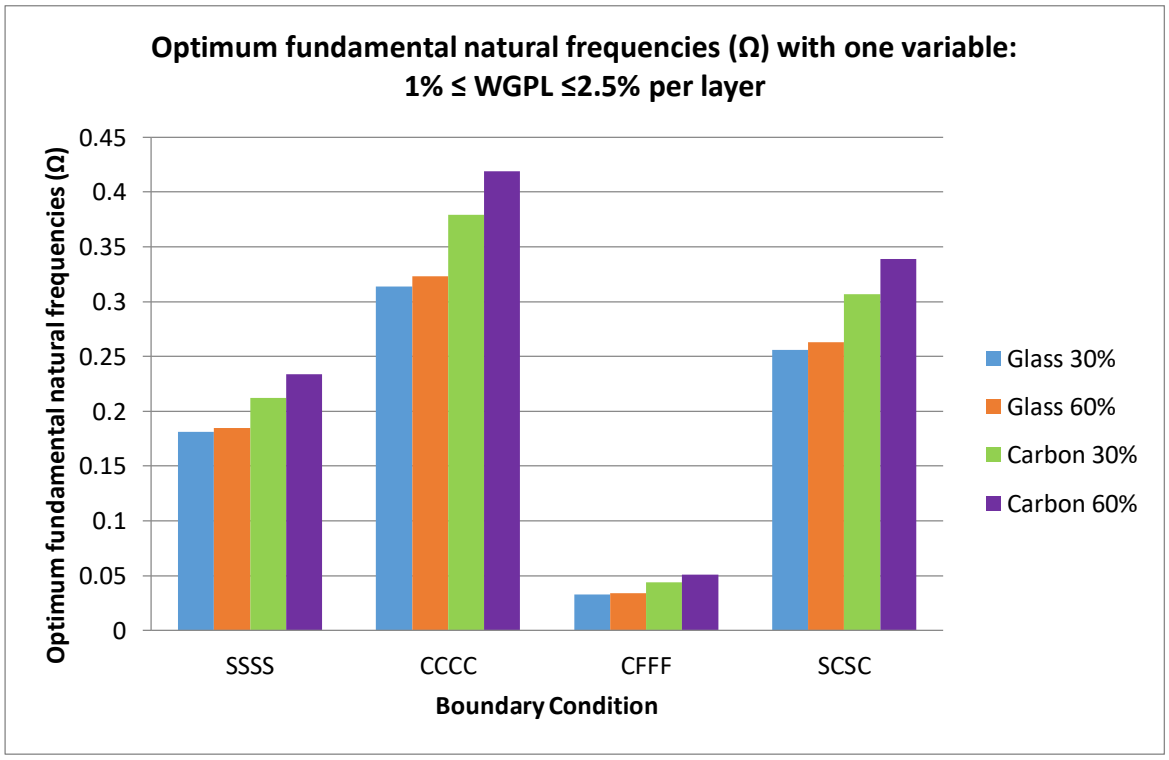

Figure 3.2.1. 6: Graphical representation of result from Table 3.2.1.2

We can see in this simulation the increase of fibre content from 30% to 60% resulted in an increase in the fundamental frequency of the laminate. Clearly, in these results, carbon fibres produced a higher fundamental frequency than glass fibres.

In Table 3.2.1.3 the effect of varying boundary conditions and graphene weight on the optimal fundamental frequency is presented, when a limit equal to 20% for the total graphene weight of the laminate is assigned (summation of graphene weight per layer is equal to 20%, Eq. (32b)).

Table 3.2.1. 3: Optimum fundamental natural frequencies (Ω), with one variable: 1% ≤ WGPL ≤10% per layer and total W_{GPL} of the laminate equal to 20%

BCs		**Optimal W_{GPL}**	**Ω**
SSSS	**Glass 30%**	[0.07 / 0.01 / 0.01 / 0.01 / 0.01 / 0.01 / 0.01 / 0.07]	0.2084
	Glass 60%	[0.058 / 0.022 / 0.01 / 0.01 / 0.01 / 0.01 / 0.022 / 0.058]	0.1979
	Carbon 30%	[0.07 / 0.01 / 0.01 / 0.01 / 0.01 / 0.01 / 0.01 / 0.07]	0.2348
	Carbon 60%	[0.061 / 0.019 / 0.01 / 0.01 / 0.01 / 0.01 / 0.019 / 0.061]	0.2429
CCCC	**Glass 30%**	[0.07 / 0.01 / 0.01 / 0.01 / 0.01 / 0.01 / 0.01 / 0.07]	0.3506
	Glass 60%	[0.058 / 0.022 / 0.01 / 0.01 / 0.01 / 0.01 / 0.022 / 0.058]	0.3385
	Carbon 30%	[0.07 / 0.01 / 0.01 / 0.01 / 0.01 / 0.01 / 0.01 / 0.07]	0.4015
	Carbon 60%	[0.051 / 0.024 / 0.015 / 0.011 / 0.011 / 0.015 / 0.024 / 0.051]	0.4238
CFFF	**Glass 30%**	[0.07 / 0.01 / 0.01 / 0.01 / 0.01 / 0.01 / 0.01 / 0.07]	0.0381
	Glass 60%	[0.064 / 0.016 / 0.01 / 0.01 / 0.01 / 0.01 / 0.016 / 0.064]	0.0361
	Carbon 30%	[0.07 / 0.01 / 0.01 / 0.01 / 0.01 / 0.01 / 0.01 / 0.07]	0.0480
	Carbon 60%	[0.07 / 0.01 / 0.01 / 0.01 / 0.01 / 0.01 / 0.01 / 0.07]	0.0522
SCSC	**Glass 30%**	[0.07 / 0.01 / 0.01 / 0.01 / 0.01 / 0.01 / 0.01 / 0.07]	0.2885
	Glass 60%	[0.058 / 0.022 / 0.01 / 0.01 / 0.01 / 0.01 / 0.022 / 0.058]	0.2774
	Carbon 30%	[0.07 / 0.01 / 0.01 / 0.01 / 0.01 / 0.01 / 0.01 / 0.07]	0.3287
	Carbon 60%	[0.054 / 0.023 / 0.012 / 0.01 / 0.01 / 0.012 / 0.023 / 0.054]	0.3450

Note: D/L = 0.1, aspect ratio = 1 and fibre stacking sequence [0/90/0/90/0/90/0/90]:

Table 3.2.1.3 shows that the outer layers of the laminate require an increased amount of graphene in respect to the inner layers, to produce the optimum fundamental frequency. For the majority of the cases of Table 3.2.1.3, only one or two outer layers (out of eight) get the increased graphene weight while the middle layers get only the minimum weight. Thus, a cost-effective design can be achieved if

the maximum graphene weight is not arbitrarily assigned to each layer. In addition, the increased graphene weight assigned to outer layers (up to 7%) is still lower than the upper limit.

For all the boundary conditions, an increase in the content of carbon fibres (from 30% to 60%) results in the increase of the fundamental frequency, contrary to the results presented in Table 3.2.1.1. However, it is noticed that similar to Table 3.2.1.1, an increase in the content of glass fibres per layer (from 30% to 60%) results in the decrease of the fundamental frequency (see Figure 3.2.1.7). Carbon fibres have stronger mechanical properties than glass and this could be the reason we see this difference in fundamental frequency when changing the fibre content from 30% to 60%. For glass fibres, we can see that increasing the fibre content also lowered the graphene content in the outer layers. The decrease in graphene could contribute to the decrease in fundamental frequency when the fibre content is increased.

Figure 3.2.1.7 shows a graphical representation of the results for Table 3.2.1.3.

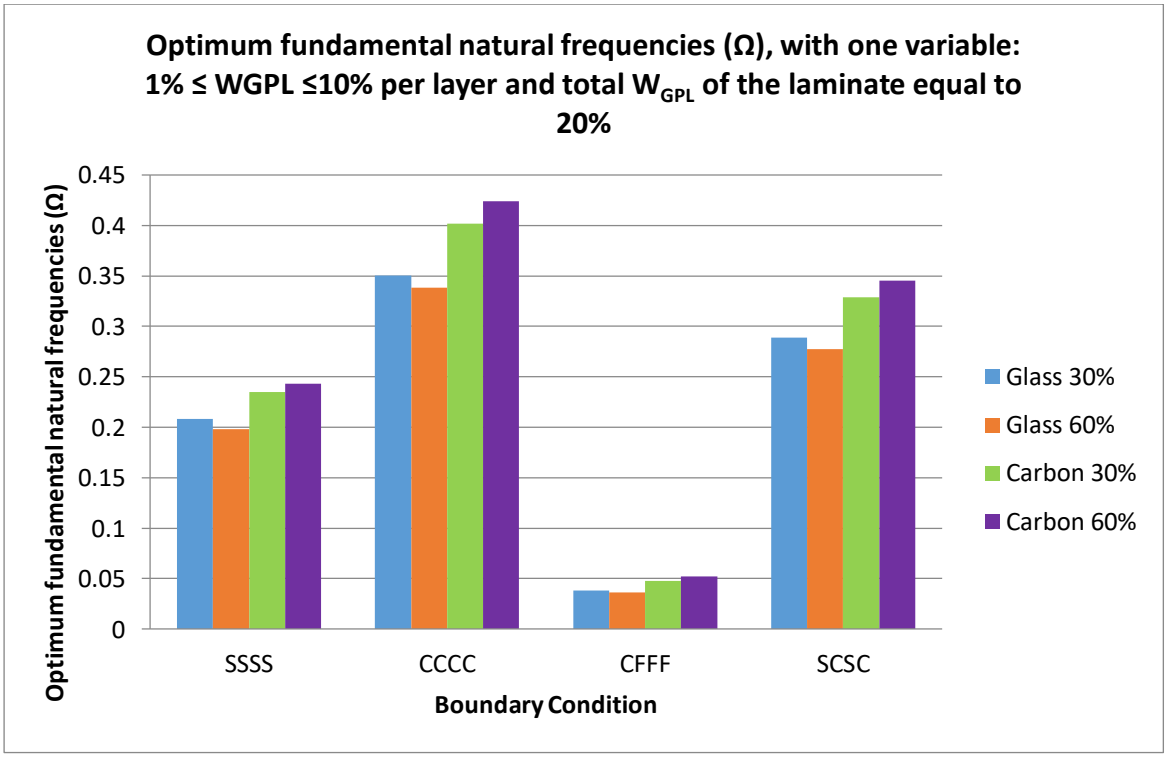

Figure 3.2.1. 7: Graphical representation of result from Table 3.2.1.3

Tables 3.2.1.4 and 3.2.1.5 present the optimal natural frequencies for the case of different total laminate thickness over edge length (D/L) ratios, when all the other parameters are the same as those presented in Table 3.2.1.3.

Table 3.2.1. 4: Optimum fundamental natural frequencies (Ω), with one variable: 1% ≤ WGPL ≤10% per layer and total W_{GPL} of the laminate equal to 20%, D/L =0.01.

BCs		Optimal W_{GPL}	Ω
		D/L = 0.01	
SSSS	**Glass 30%**	[0.07 / 0.01 / 0.01 / 0.01 / 0.01 / 0.01 / 0.01 / 0.07]	0.0022
	Glass 60%	[0.06 / 0.02 / 0.01 / 0.01 / 0.01 / 0.01 / 0.02 / 0.06]	0.0021
	Carbon 30%	[0.07 / 0.01 / 0.01 / 0.01 / 0.01 / 0.01 / 0.01 / 0.07]	0.0025
	Carbon 60%	[0.064 / 0.016 / 0.01 / 0.01 / 0.01 / 0.01 / 0.016 / 0.06]	0.0026
CCCC	**Glass 30%**	[0.07 / 0.01 / 0.01 / 0.01 / 0.01 / 0.01 / 0.01 / 0.07]	0.0041
	Glass 60%	[0.062 / 0.018 / 0.01 / 0.01 / 0.01 / 0.01 / 0.018 / 0.062]	0.0038
	Carbon 30%	[0.07 / 0.01 / 0.01 / 0.01 / 0.01 / 0.01 / 0.01 / 0.07]	0.0049
	Carbon 60%	[0.07 / 0.01 / 0.01 / 0.01 / 0.01 / 0.01 / 0.01 / 0.07]	0.0053
CFFF	**Glass 30%**	[0.055 / 0.025 / 0.01 / 0.01 / 0.01 / 0.01 / 0.025 / 0.055]	0.00038
	Glass 60%	[0.031 / 0.027 / 0.018 / 0.024 / 0.024 / 0.018 / 0.027 / 0.031]	0.00034
	Carbon 30%	[0.055 / 0.025 / 0.01 / 0.01 / 0.01 / 0.01 / 0.025 / 0.055]	0.00046
	Carbon 60%	[0.031 / 0.027 / 0.018 / 0.024 / 0.024 / 0.018 / 0.027 / 0.031]	0.00052
SCSC	**Glass 30%**	[0.07 / 0.01 / 0.01 / 0.01 / 0.01 / 0.01 / 0.01 / 0.07]	0.0033
	Glass 60%	[0.061 / 0.019 / 0.01 / 0.01 / 0.01 / 0.01 / 0.019 / 0.061]	0.0031
	Carbon 30%	[0.07 / 0.01 / 0.01 / 0.01 / 0.01 / 0.01 / 0.01 / 0.07]	0.0039
	Carbon 60%	[0.069 / 0.011 / 0.01 / 0.01 / 0.01 / 0.01 / 0.011 / 0.069]	0.0041

Note: aspect ratio = 1 and fibre stacking sequence [0/90/0/90/0/90/0/90]:

Table 3.2.1. 5: Optimum fundamental natural frequencies (Ω), with one variable: 1% ≤ WGPL ≤10% per layer and total W_{GPL} of the laminate equal to 20%, D/L =0.2.

BCs		Optimal W_{GPL}	Ω
		D/L = 0.2	
SSSS	**Glass 30%**	[0.069 / 0.011 / 0.01 / 0.01 / 0.01 / 0.01 / 0.011 / 0.069]	0.7379
	Glass 60%	[0.056 / 0.024 / 0.01 / 0.01 / 0.01 / 0.01 / 0.024 / 0.056]	0.7132
	Carbon 30%	[0.07 / 0.01 / 0.01 / 0.01 / 0.01 / 0.01 / 0.01 / 0.07]	0.8076
	Carbon 60%	[0.053 / 0.024 / 0.013 / 0.01 / 0.01 / 0.013 / 0.024 / 0.053]	0.8337
CCCC	**Glass 30%**	[0.061 / 0.019 / 0.01 / 0.01 / 0.01 / 0.01 / 0.019 / 0.061]	1.071
	Glass 60%	[0.048 / 0.026 / 0.015 / 0.011 / 0.011 / 0.015 / 0.026 / 0.048]	1.068
	Carbon 30%	[0.055 / 0.022 / 0.013 / 0.01 / 0.01 / 0.013 / 0.022 / 0.055]	1.151
	Carbon 60%	[0.033 / 0.026 / 0.021 / 0.02 / 0.02 / 0.021 / 0.026 / 0.033]	1.209
CFFF	**Glass 30%**	[0.07 / 0.01 / 0.01 / 0.01 / 0.01 / 0.01 / 0.01 / 0.07]	0.1467
	Glass 60%	[0.063 / 0.017 / 0.01 / 0.01 / 0.01 / 0.01 / 0.017 / 0.063]	0.1399
	Carbon 30%	[0.07 / 0.01 / 0.01 / 0.01 / 0.01 / 0.01 / 0.01 / 0.07]	0.1818
	Carbon 60%	[0.066 / 0.014 / 0.01 / 0.01 / 0.01 / 0.01 / 0.014 / 0.066]	0.1967
SCSC	**Glass 30%**	[0.063 / 0.017 / 0.01 / 0.01 / 0.01 / 0.01 / 0.017 / 0.063]	0.9122
	Glass 60%	[0.05 / 0.026 / 0.014 / 0.01 / 0.01 / 0.014 / 0.026 / 0.05]	0.9024
	Carbon 30%	[0.061 / 0.019 / 0.01 / 0.01 / 0.01 / 0.01 / 0.019 / 0.061]	0.9849
	Carbon 60%	[0.039 / 0.026 / 0.019 / 0.016 / 0.016 / 0.019 / 0.026 / 0.039]	1.0287

Note: aspect ratio = 1 and fibre stacking sequence [0/90/0/90/0/90/0/90]:

As expected, an increase in the D/L ratio of the laminate results in the increase of the optimum fundamental frequency (Figure 3.2.1.8 and 3.2.1.9). In addition, similar to Table 3.2.1.3, for the majority of the simulations the outer layers require more graphene than the inner layers while an increase of the glass fibre content reduces the natural frequency. Again the increase in glass fibres leads to a decrease in graphene in the outer layers and ultimately a decrease in fundamental frequency. It is worth noticing that from Tables 3.2.1.3, 3.2.1.4 and 3.2.1.5 the highest value for the graphene weight is equal to 7%, which corresponds to the top and bottom (1st and 8th) layers of the laminate. The second higher value of optimal graphene weight is 2.7% for the 2nd and 6th layer while for all the other layers, a lower graphene weight is obtained. Figure 3.2.1.8 and 3.2.1.9 shows the graphical representation of the results in Table 3.2.1.4 and 3.2.1.5.

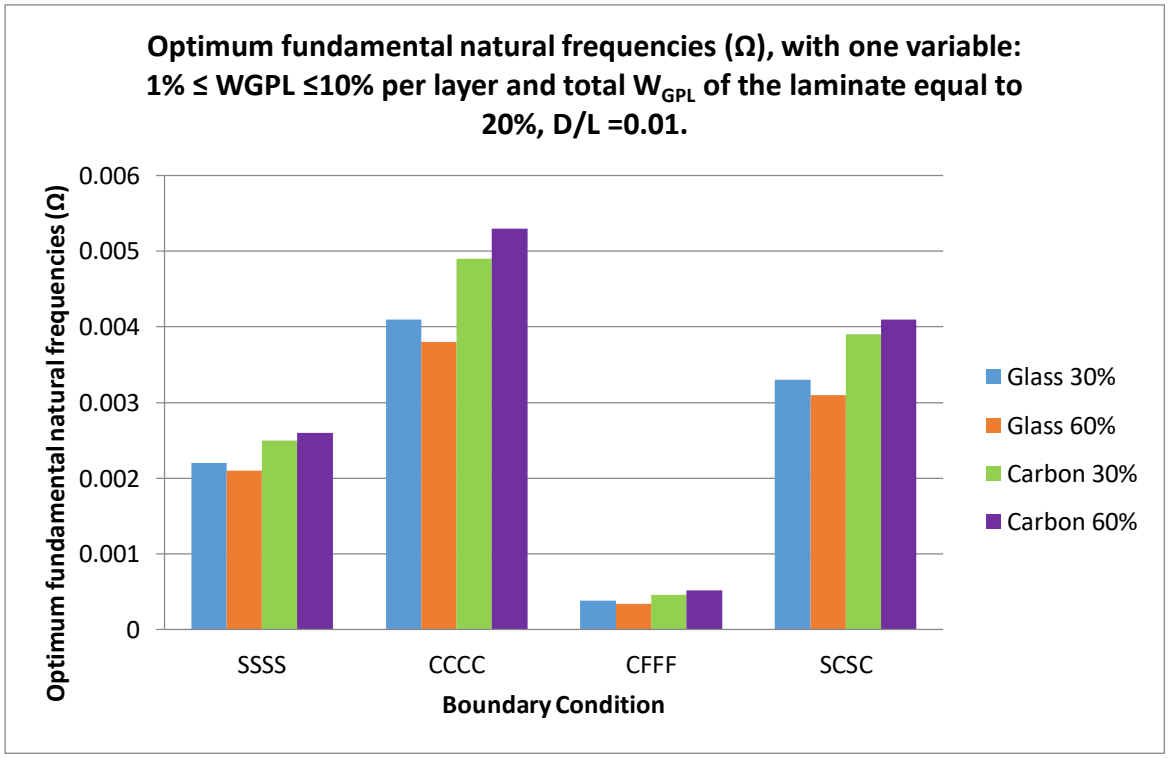

Figure 3.2.1. 8: Graphical representation of result from Table 3.2.1.4

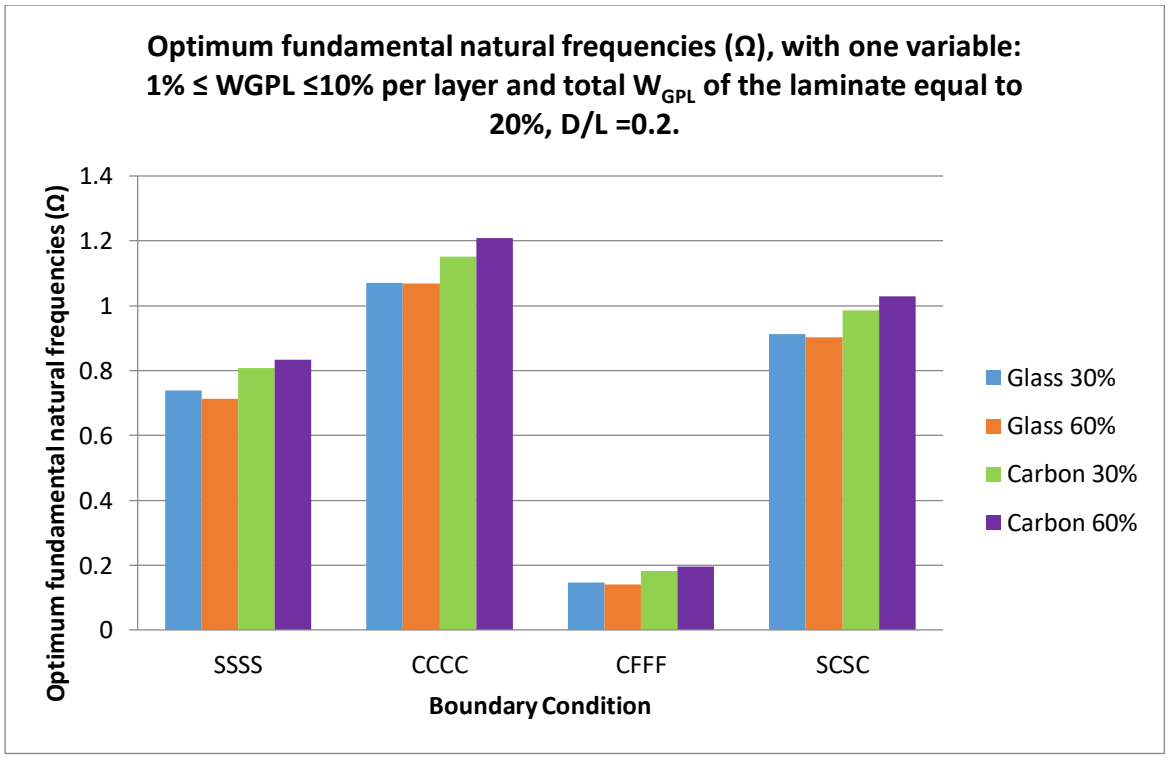

Figure 3.2.1. 9: Graphical representation of result from Table 3.2.1.5

Similar results regarding maximum graphene weights in the outer and middle layers are received in Table 3.2.1.6 for different aspect ratios and the SSSS boundary condition.

Table 3.2.1. 6: Optimum fundamental natural frequencies (Ω), with one variable: 1% ≤ WGPL ≤10% per layer and total W_{GPL} of the laminate equal to 20% and varying aspect ratio.

BCs		Optimal W_{GPL}	Ω
		Aspect ratio = 1	
SSSS	**Glass 30%**	[0.07 / 0.01 / 0.01 / 0.01 / 0.01 / 0.01 / 0.01 / 0.07]	0.2084
	Glass 60%	[0.058 / 0.022 / 0.01 / 0.01 / 0.01 / 0.01 / 0.022 / 0.058]	0.1979
	Carbon 30%	[0.07 / 0.01 / 0.01 / 0.01 / 0.01 / 0.01 / 0.01 / 0.07]	0.2348
	Carbon 60%	[0.061 / 0.019 / 0.01 / 0.01 / 0.01 / 0.01 / 0.019 / 0.061]	0.2429
		Aspect ratio = 1.5	
SSSS	**Glass 30%**	[0.07 / 0.01 / 0.01 / 0.01 / 0.01 / 0.01 / 0.01 / 0.07]	0.3297
	Glass 60%	[0.058 / 0.022 / 0.01 / 0.01 / 0.01 / 0.01 / 0.022 / 0.058]	0.3145
	Carbon 30%	[0.07 / 0.01 / 0.01 / 0.01 / 0.01 / 0.01 / 0.01 / 0.07]	0.3732
	Carbon 60%	[0.059 / 0.021 / 0.01 / 0.01 / 0.01 / 0.01 / 0.021 / 0.059]	0.3882
		Aspect ratio = 2	
SSSS	**Glass 30%**	[0.07 / 0.01 / 0.01 / 0.01 / 0.01 / 0.01 / 0.01 / 0.07]	0.4899
	Glass 60%	[0.058 / 0.022 / 0.01 / 0.01 / 0.01 / 0.01 / 0.022 / 0.058]	0.4697
	Carbon 30%	[0.07 / 0.01 / 0.01 / 0.01 / 0.01 / 0.01 / 0.01 / 0.07]	0.5574
	Carbon 60%	[0.056 / 0.023 / 0.011 / 0.01 / 0.01 / 0.011 / 0.023 / 0.056]	0.5834

Note: D/L = 0.1 and fibre stacking sequence [0/90/0/90/0/90/0/90]:

The increase in aspect ratio results in higher fundamental frequencies for both glass and carbon. Inspecting the results of Table 3.2.1.6 shows increasing the aspect ratio resulted in the same trends such as: increasing the glass fibres lowers the required graphene needed in the outer layers, resulting in a decrease in fundamental frequency; Increasing the carbon fibre content leads to lower graphene needed in the outer layers and an increase in the fundamental frequency (This result can be seen in Table 3.2.1.3 to Table 3.2.1.6).

Refer to Figure 3.2.1.6 for a graphical representation of the results.

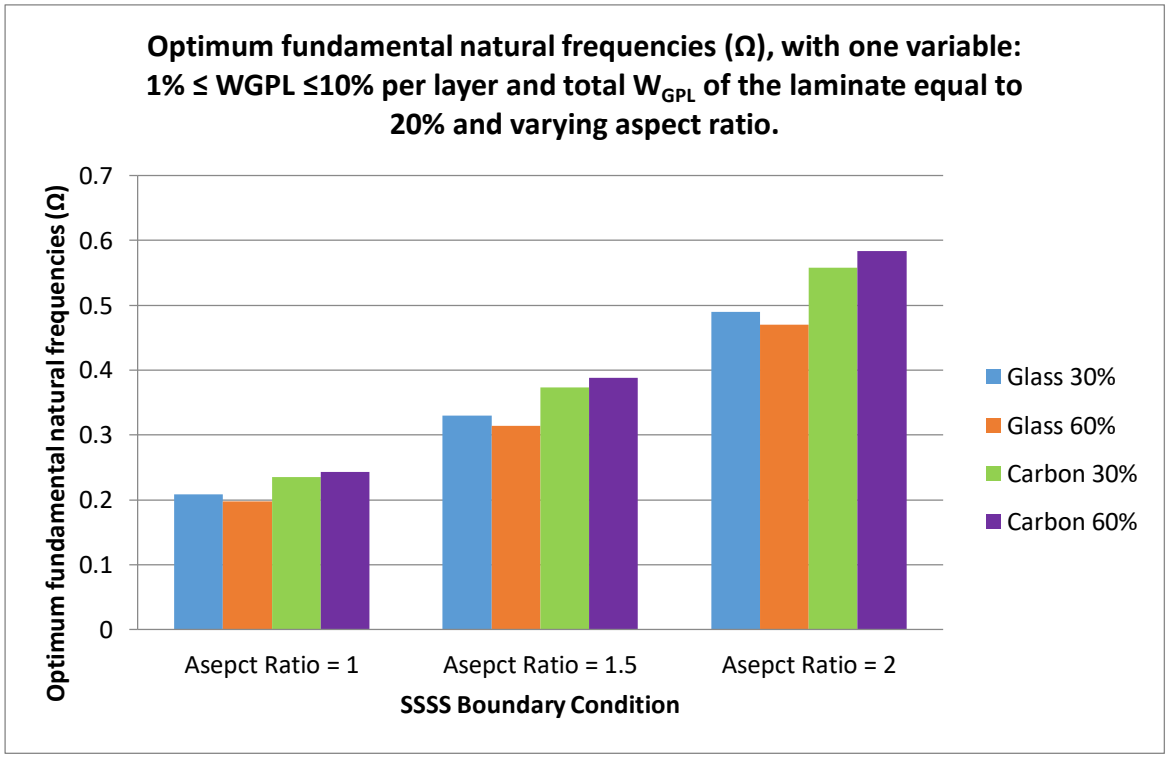

Figure 3.2.1. 10: Graphical representation of result from Table 3.2.1.6

To further investigate the optimal distribution of graphene on the laminate, the limits of graphene weight are reduced. For the minimum limit, simulations with values equal to 0.1% and 1% are considered, while for the maximum limit a value equal to 2.5% is set. In addition, the summation of graphene weight for all layers of the laminate is equal to 10%. In Table 3.2.1.7, the corresponding natural frequencies are presented for SSSS boundary condition.

Table 3.2.1. 7: Optimum fundamental Ω with one variable: W_{GPL} between 0.1% or 1% and 2.5% per layer, total W_{GPL} of the laminate equal to 10%.

BCs		Optimal W_{GPL}	Ω
		Graphene weight between 0.1% and 2.5%	
SSSS	**Glass 30%**	[0.025 / 0.023 / 0.001 / 0.001 / 0.001 / 0.001 / 0.023 / 0.025]	0.1686
	Glass 60%	[0.025 / 0.021 / 0.003 / 0.001 / 0.001 / 0.003 / 0.021 / 0.025]	0.1753
	Carbon 30%	[0.025 / 0.023 / 0.001 / 0.001 / 0.001 / 0.001 / 0.023 / 0.025]	0.1996
	Carbon 60%	[0.025 / 0.018 / 0.006 / 0.001 / 0.001 / 0.006 / 0.018 / 0.025]	0.2247
		Graphene weight between 1% and 2.5%	
SSSS	**Glass 30%**	[0.02 / 0.01 / 0.01 / 0.01 / 0.01 / 0.01 / 0.01 / 0.02]	0.1563
	Glass 60%	[0.02 / 0.01 / 0.01 / 0.01 / 0.01 / 0.01 / 0.01 / 0.02]	0.1683
	Carbon 30%	[0.02 / 0.01 / 0.01 / 0.01 / 0.01 / 0.01 / 0.01 / 0.02]	0.1913
	Carbon 60%	[0.02 / 0.01 / 0.01 / 0.01 / 0.01 / 0.01 / 0.01 / 0.02]	0.2214

Note: D/L = 0.1, aspect ratio = 1 and fibre stacking sequence [0/90/0/90/0/90/0/90]:

According to the results shown in Table 3.2.1.7, the minimum limit of graphene weight of 0.1% allows for an optimal distribution of graphene which results in higher natural frequencies, in comparison with the case of 1% minimum graphene limit. The reason for this is that the lower minimum limit allows for higher reinforcement on two top and two bottom surface layers, while the intermediate layers get only the minimum quantity (0.1%). In addition, according to Table 3.2.1.7 and contrary to all previous results, increase of glass fibre content results in the increase of the natural frequency. Similar results are obtained for the other boundary conditions. The difference in this result for glass is the outer layers having the maximum allowable graphene content in both fibre content cases, whereas previously, increasing the fibre content of glass decreased the graphene content in the outer layers.

Refer to Figure 3.2.1.11 for a graphical representation of the results.

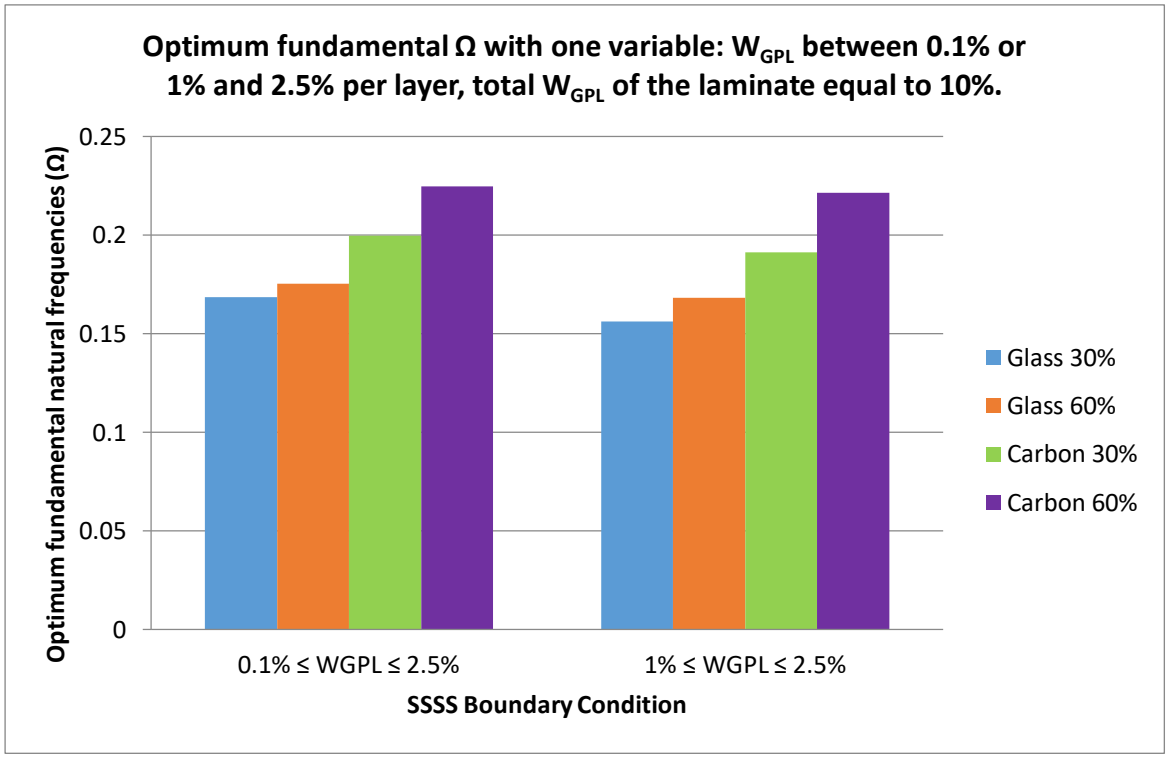

Figure 3.2.1. 11: Graphical representation of result from Table 3.2.1.7

The resultant decrease in fundamental frequency when changing the minimum limit of graphene from 0.1% to 1%, fall in a range of 1.47% to 7.30% with the largest change being for glass fibres at 30%.

3.2.2 Influence of graphene weight, fibre content, thickness ratio and stacking sequence on natural vibration

Firstly, in Table 3.2.2.1 two design variables are adopted, namely the graphene weight (W_{GPL}) and the fibre content (V_F). Then, the thickness ratio and the fibre angles are also considered as additional design variables.

Table 3.2.2. 1: Optimum fundamental natural frequencies (Ω) with two variables: W_{GPL} and V_F

BCs		**Optimal W_{GPL}**	**Optimal Fibre Content V_F**	**Ω**
		$0.1\% \le W_{GPL} \le 2.5\%$ per layer	$10\% \le V_F \le 60\%$ per layer	
SSSS	**Glass**	[0.025 / 0.023 / 0.001 / 0.001 / 0.001 / 0.001 / 0.023 / 0.025]	[0.6 / 0.6 / 0.1 / 0.1 / 0.1 / 0.1 / 0.6 / 0.6]	0.1860
	Carbon	[0.025 / 0.018 / 0.006 / 0.001 / 0.001 / 0.006 / 0.018 / 0.025]	[0.6 / 0.6 / 0.6 / 0.1 / 0.1 / 0.6 / 0.6 / 0.6]	0.2259
CCCC	**Glass**	[0.025 / 0.023 / 0.001 / 0.001 / 0.001 / 0.001 / 0.023 / 0.025]	[0.6 / 0.6 / 0.1 / 0.1 / 0.1 / 0.1 / 0.6 / 0.6]	0.3135
	Carbon	[0.021 / 0.013 / 0.009 / 0.007 / 0.007 / 0.009 / 0.013 / 0.021]	[0.6 / 0.6 / 0.6 / 0.6 / 0.6 / 0.6 / 0.6 / 0.6]	0.3913
CFFF	**Glass**	[0.025 / 0.023 / 0.001 / 0.001 / 0.001 / 0.001 / 0.023 / 0.025]	[0.6 / 0.6 / 0.1 / 0.1 / 0.1 / 0.1 / 0.6 / 0.6]	0.0345
	Carbon	[0.025 / 0.018 / 0.006 / 0.001 / 0.001 / 0.006 / 0.018 / 0.025]	[0.6 / 0.6 / 0.3 / 0.3 / 0.3 / 0.3 / 0.6 / 0.6]	0.0501
SCSC	**Glass**	[0.025 / 0.023 / 0.001 / 0.001 / 0.001 / 0.001 / 0.023 / 0.025]	[0.6 / 0.6 / 0.1 / 0.1 / 0.1 / 0.1 / 0.6 / 0.6]	0.2578
	Carbon	[0.024 / 0.013 / 0.008 / 0.005 / 0.005 / 0.008 / 0.013 / 0.024]	[0.6 / 0.6 / 0.6 / 0.6 / 0.6 / 0.6 / 0.6 / 0.6]	0.3183

Note: D/L = 0.1, aspect ratio = 1, fibre stacking sequence [0/90/0/90/0/90/0/90] and total W_{GPL} of the laminate equal to 10%

According to Table 3.2.2.1, a higher optimal graphene weight for the outer than the middle layers arises for the four boundary conditions. For carbon fibres in the CCCC and SCSC boundary conditions, the middle layers are assigned higher than the

minimum graphene weights while for SSSS and CFFF the minimum graphene weight is obtained for the middle layers.

Taking into account the optimal fibre content distribution in the layers of the laminate, all boundary conditions result in a higher optimal fibre content for the outer layers than the middle layers, which are assigned the minimum quantity of reinforcement, for glass fibres. However, for carbon fibres this is the case only for SSSS, since for the three remaining boundary conditions, the carbon fibre content for the middle layers is greater than the minimum quantity or equal to the maximum quantity.

In addition, comparison between optimal frequencies for SSSS presented in Tables 3.2.1.7 and 3.2.2.1 indicates that a higher frequency can be obtained without using the maximum fibre content in all the layers (Table 3.2.2.1), contrary to the case where the maximum fibre content is assigned for every layer (Table 3.2.1.7). Figure 3.2.2.1 shows a graphical representation of the results.

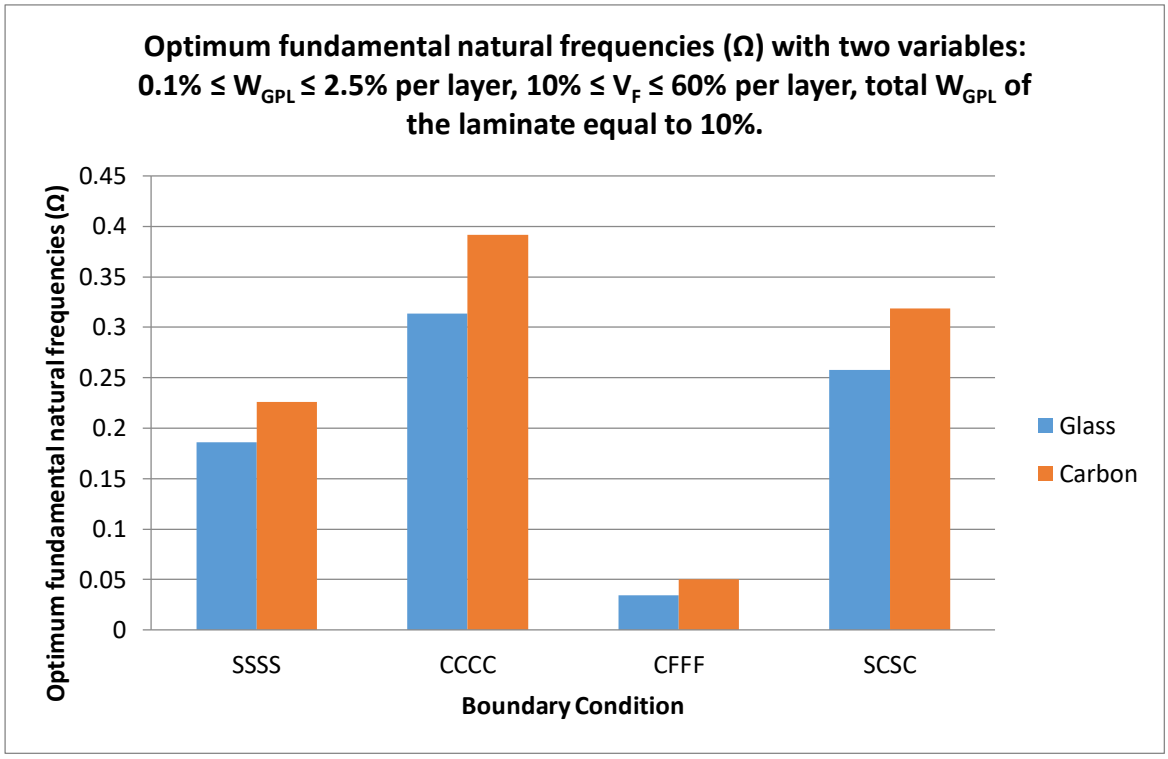

Figure 3.2.2. 1: Graphical representation of result from Table 3.2.2.1

To investigate the influence of graphene on the optimal natural vibration, additional simulations with zero graphene quantity have been performed.

Results shown in Table 3.2.2.2 indicate that for the majority of the simulations, the maximum content of fibres for every layer arises in the optimal solution. Furthermore, the optimal natural vibrations are reduced in a range between 9% and 39% in respect to those received from the graphene/fibre reinforced laminate shown in Table 3.2.2.1. This result, from Table 3.2.2.2, is attributed to zero graphene added to the laminate, indicating that even a small quantity of graphene as presented in Table 3.2.2.1., can significantly improve the vibration response, by increasing the fundamental frequency.

The observed reductions of the fundamental frequency for zero graphene are higher for glass fibres, compared to carbon fibres, which is expected due to lower mechanical properties of glass, relative to carbon fibres. Carbon fibres have a higher Young's modulus and Shear modulus than glass which explains why the reductions are higher for glass than carbon fibres. The lowest reduction arises for the CFFF laminate, which is less restrained than the other boundary conditions.

In all boundary conditions carbon fibres produced a higher fundamental frequency than glass fibres (see Figure 3.2.2.2). The increase in fundamental frequency is 36.74%, 31.07%, 44.27% and 32.82% for SSSS, CCCC, CFFF and SCSC respectively when the fibre is changed from glass to carbon.

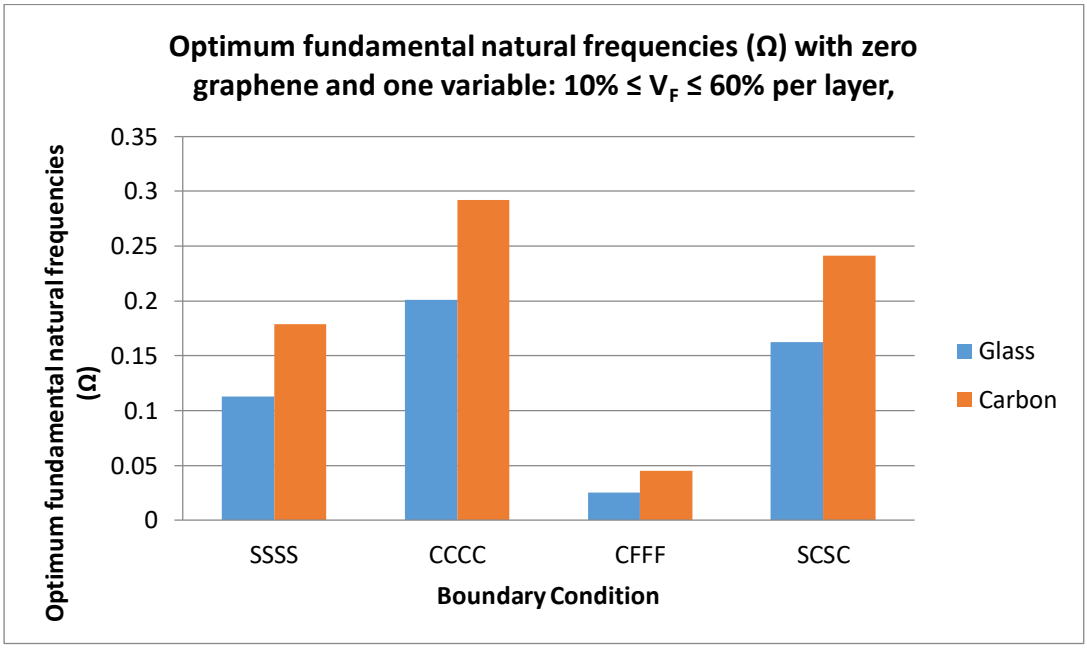

Figure 3.2.2. 2: Graphical representation of result from Table 3.2.2.2

Table 3.2.2.2: Optimum fundamental natural frequencies (Ω) with zero graphene and one variable: VF

BCs		Optimal V_F	Ω
		10% ≤ V_F ≤ 60% per layer	
SSSS	Glass	[0.6 / 0.6 / 0.6 / 0.1 / 0.1 / 0.6 / 0.6 / 0.6]	0.1131
	Carbon	[0.6 / 0.6 / 0.6 / 0.6 / 0.6 / 0.6 / 0.6 / 0.6]	0.1788
CCCC	Glass	[0.6 / 0.6 / 0.6 / 0.6 / 0.6 / 0.6 / 0.6 / 0.6]	0.2012
	Carbon	[0.6 / 0.6 / 0.6 / 0.6 / 0.6 / 0.6 / 0.6 / 0.6]	0.2919
CFFF	Glass	[0.6 / 0.6 / 0.1 / 0.1 / 0.1 / 0.1 / 0.6 / 0.6]	0.0253
	Carbon	[0.6 / 0.6 / 0.6 / 0.6 / 0.6 / 0.6 / 0.6 / 0.6]	0.0454
SCSC	Glass	[0.6 / 0.6 / 0.6 / 0.6 / 0.6 / 0.6 / 0.6 / 0.6]	0.1623
	Carbon	[0.6 / 0.6 / 0.6 / 0.6 / 0.6 / 0.6 / 0.6 / 0.6]	0.2416

Note: D/L = 0.1, aspect ratio = 1 and fibre stacking sequence [0/90/0/90/0/90/0/90]:

In Tables 3.2.2.3 to 3.2.2.6 results from simulations with the four boundary conditions (BCs) and different stacking sequences are presented, from the model with three design variables, namely graphene weight, fibre content (glass or carbon) and thickness ratio (layer thickness over overall laminate thickness ratio, h/D). Figure 3.2.2.3 to Figure 3.2.2.6 illustrates the results in a graphical format.

The goal of these simulations is to depict how a non-uniform layer thickness influences the results for the eight-layered composite.

Table 3.2.2.3: Optimum fundamental natural frequencies (Ω)with three variables: WGPL ,VF and h/D for SSSS Boundary Condition.

Stacking sequence		**Optimal W_{GPL}**	**Optimal V_F**	**h_i/D**	**Ω**
		$0.1\% \le W_{GPL} \le 2.5\%$ per layer	$10\% \le V_F \le 60\%$ per layer	$0.01 \le h/D \le 0.15$ per layer	
[0/90/0/90/0/ 90/0/90]	**Glass**	[0.025/0.023/0.001/0.001/ 0.001/0.001/0.023/0.025]	[0.6/0.6/0.1/0.1/ 0.1/0.1/0.6/0.6]	[0.15/0.15/0.05/0.15/ 0.15/0.05/0.15/0.15]	0.0219
	Carbon	[0.025/0.023/0.001/0.001/ 0.001/0.001/0.023/0.025]	[0.6/0.6/0.1/0.1/ 0.1/0.1/0.6/0.6]	[0.14/0.15/0.06/0.15/ 0.15/0.06/0.15/0.14]	0.0276
[90/0/90/0/0/ 90/0/90]	**Glass**	[0.025/0.023/0.001/0.001/ 0.001/0.001/0.023/0.025]	[0.6/0.6/0.1/0.1/ 0.1/0.1/0.6/0.6]	[0.15/0.15/0.09/0.11/ 0.11/0.09/0.15/0.15]	0.0219
	Carbon	[0.025/0.023/0.001/0.001/ 0.001/0.001/0.023/0.025]	[0.6/0.6/0.6/0.1/ 0.1/0.6/0.6/0.6]	[0.15/0.15/0.05/0.15/ 0.15/0.05/0.15/0.15]	0.0278
[45/45/45/45/ 45/45/45/45]	**Glass**	[0.025/0.023/0.001/0.001/ 0.001/0.001/0.023/0.025]	[0.6/0.6/0.1/0.1/ 0.1/0.1/0.6/0.6]	[0.15/0.15/0.05/0.15/ 0.15/0.05/0.15/0.15]	0.0223
	Carbon	[0.025/0.023/0.001/0.001/ 0.001/0.001/0.023/0.025]	[0.6/0.6/0.6/0.1/ 0.1/0.6/0.6/0.6]	[0.15/0.15/0.05/0.15/ 0.15/0.05/0.15/0.15]	0.0288
[45/90/45/90/ 45/90/45/90]	**Glass**	[0.025/0.023/0.001/0.001/ 0.001/0.001/0.023/0.025]	[0.6/0.6/0.1/0.1/ 0.1/0.1/0.6/0.6]	[0.15/0.15/0.1/0.1/0.1 /0.1/0.15/0.15]	0.0221
	Carbon	[0.025/0.023/0.001/0.001/ 0.001/0.001/0.023/0.025]	[0.6/0.6/0.1/0.1/ 0.1/0.1/0.6/0.6]	[0.15/0.15/0.05/0.15/ 0.15/0.05/0.15/0.15]	0.0292
[45/90/45/90/ 90/45/90/45]	**Glass**	[0.025/0.023/0.001/0.001/ 0.001/0.001/0.023/0.025]	[0.6/0.6/0.1/0.1/ 0.1/0.1/0.6/0.6]	[0.15/0.15/0.15/0.05/ 0.05/0.15/0.15/0.15]	0.0222
	Carbon	[0.025/0.023/0.001/0.001/ 0.001/0.001/0.023/0.025]	[0.6/0.6/0.6/0.1/ 0.1/0.6/0.6/0.6]	[0.15/0.15/0.05/0.15/ 0.15/0.05/0.15/0.15]	0.0294
[30/90/45/60/ 60/45/90/30]	**Glass**	[0.025/0.023/0.001/0.001/ 0.001/0.001/0.023/0.025]	[0.6/0.6/0.1/0.1/ 0.1/0.1/0.6/0.6]	[0.15/0.15/0.15/0.05/ 0.05/0.15/0.15/0.15]	0.0221
	Carbon	[0.025/0.023/0.001/0.001/ 0.001/0.001/0.023/0.025]	[0.6/0.6/0.6/0.1/ 0.1/0.6/0.6/0.6]	[0.15/0.15/0.05/0.15/ 0.15/0.05/0.15/0.15]	0.0290

Note: D/L = 0.1, aspect ratio = 1 and total W_{GPL} of the laminate equal to 10%

The results in Table 3.2.2.3 are for the SSSS (simply supported) boundary conditions. It is noticed that changing glass to carbon increased the fundamental frequency in a range of 20.65% to 24.49%.

The largest fundamental frequency produced was 0.0294 which utilized carbon fibres with a stacking sequence of [45/90/45/90/90/45/90/45]. For glass the largest fundamental frequency was 0.0223 with the [45/45/45/45/45/45/45/45] stacking sequence.

Referring to Figure 3.2.2.3, we can see the fundamental frequency for different stacking sequences produced similar results.

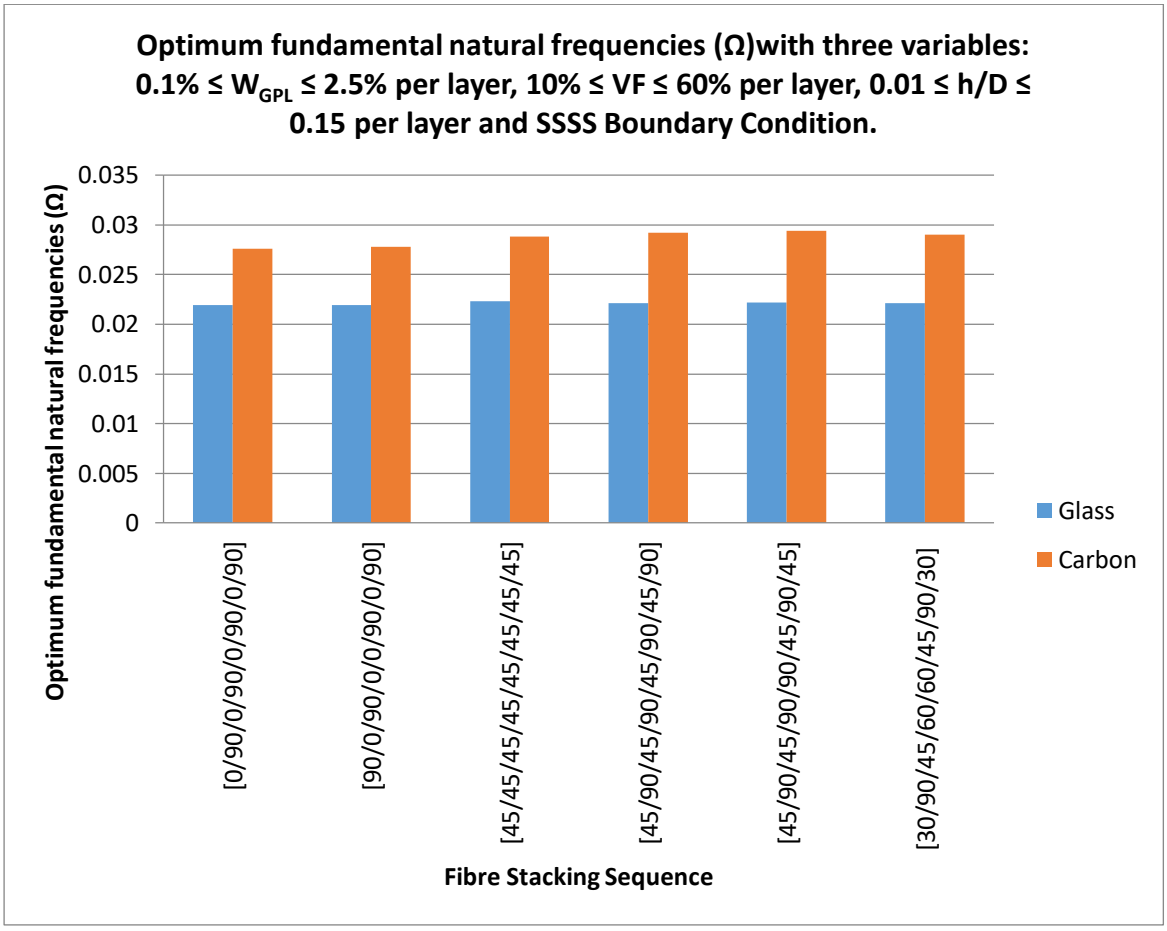

Figure 3.2.2. 3: Graphical representation of result from Table 3.2.2.3

For glass fibres the largest variance of the fundamental frequency is 1.79% (0.0219 to 0.0223) and for carbon it is 6.12% (0.0276 to 0.0294).

All simulations in Table 3.2.2.3 required the maximum distribution of graphene in the outer layers (2.5%) which decreased in the middle layers to the minimum value of 1%. A similar result can be seen for the fibre content with the maximum distribution of 60% in the outer layers and in the middle layers, the minimum of 10%. Analysis of the thickness produced similar results to graphene and fibre distributions.

The results in Table 3.2.2.4 are for the CCCC (clamped) boundary condition.
Immediately we notice that changing glass to carbon, again, increased the fundamental frequency in a range of 23.20% to 30.58%. This is a larger range then for the SSSS boundary condition.

Table 3.2.2.4: Optimum fundamental natural frequencies (Ω)with three variables: W_{GPL} , V_F and h/D for CCCC Boundary Condition.

Stacking sequence		**Optimal W_{GPL}**	**Optimal V_F**	**h_i/D**	**Ω**
		$0.1\% \le W_{GPL} \le 2.5\%$ per layer	$10\% \le V_F \le 60\%$ per layer	$0.01 \le h/D \le 0.15$ per layer	
[0/90/0/90/0/90/0/90]	**Glass**	[0.015/0.025/0.009/0.001/0.001/0.009/0.025/0.015]	[0.6/0.6/0.6/0.1/0.1/0.6/0.6/0.6]	[0.05/0.15/0.15/0.15/0.15/0.15/0.15/0.05]	0.0386
	Carbon	[0.025/0.023/0.001/0.001/0.001/0.001/0.023/0.025]	[0.6/0.6/0.6/0.1/0.1/0.6/0.6/0.6]	[0.12/0.15/0.08/0.15/0.15/0.08/0.15/0.12]	0.0550
[90/0/90/0/0/90/0/90]	**Glass**	[0.015/0.025/0.009/0.001/0.001/0.009/0.025/0.015]	[0.6/0.6/0.6/0.1/0.1/0.6/0.6/0.6]	[0.05/0.15/0.15/0.15/0.15/0.15/0.15/0.05]	0.0386
	Carbon	[0.025/0.023/0.001/0.001/0.001/0.001/0.023/0.025]	[0.6/0.6/0.6/0.1/0.1/0.6/0.6/0.6]	[0.15/0.15/0.05/0.15/0.15/0.05/0.15/0.15]	0.0556
[45/45/45/45/45/45/45/45]	**Glass**	[0.015/0.025/0.009/0.001/0.001/0.009/0.025/0.015]	[0.6/0.6/0.6/0.1/0.1/0.6/0.6/0.6]	[0.05/0.15/0.15/0.15/0.15/0.15/0.15/0.05]	0.0384
	Carbon	[0.025/0.023/0.001/0.001/0.001/0.001/0.023/0.025]	[0.6/0.6/0.6/0.1/0.1/0.6/0.6/0.6]	[0.15/0.15/0.05/0.15/0.15/0.05/0.15/0.15]	0.0500
[45/90/45/90/45/90/45/90]	**Glass**	[0.015/0.025/0.009/0.001/0.001/0.009/0.025/0.015]	[0.6/0.6/0.6/0.1/0.1/0.6/0.6/0.6]	[0.05/0.15/0.15/0.15/0.15/0.15/0.15/0.05]	0.0385
	Carbon	[0.025/0.023/0.001/0.001/0.001/0.001/0.023/0.025]	[0.6/0.6/0.1/0.1/0.1/0.1/0.6/0.6]	[0.15/0.15/0.05/0.15/0.15/0.05/0.15/0.15]	0.0535
[45/90/45/90/90/45/90/45]	**Glass**	[0.015/0.025/0.009/0.001/0.001/0.009/0.025/0.015]	[0.6/0.6/0.6/0.1/0.1/0.6/0.6/0.6]	[0.05/0.15/0.15/0.15/0.15/0.15/0.15/0.05]	0.0385
	Carbon	[0.012/0.025/0.012/0.001/0.001/0.012/0.025/0.012]	[0.6/0.6/0.6/0.1/0.1/0.6/0.6/0.6]	[0.05/0.15/0.15/0.15/0.15/0.15/0.15/0.05]	0.0532
[30/90/45/60/60/45/90/30]	**Glass**	[0.015/0.025/0.009/0.001/0.001/0.009/0.025/0.015]	[0.6/0.6/0.6/0.1/0.1/0.6/0.6/0.6]	[0.05/0.15/0.15/0.15/0.15/0.15/0.15/0.05]	0.0385
	Carbon	[0.025/0.023/0.001/0.001/0.001/0.001/0.023/0.025]	[0.6/0.6/0.6/0.1/0.1/0.6/0.6/0.6]	[0.14/0.15/0.06/0.15/0.15/0.06/0.15/0.14]	0.0533

Note: D/L = 0.1, aspect ratio = 1 and total W_{GPL} of the laminate equal to 10%

The largest fundamental frequency produced was 0.0556 which utilized carbon fibres with a stacking sequence of [90/0/90/0/0/90/0/90]. For glass the largest fundamental frequency was 0.0386 with the [0/90/0/90/0/90/0/90] and [90/0/90/0/0/90/0/90] stacking sequence. Interestingly we see for the glass fibres, the fundamental frequency values are almost identical for different stacking sequences.

All simulations in Table 3.2.2.4 for carbon fibres, except the [45/90/45/90/90/45/90/45] stacking sequence, required the maximum distribution of graphene in the outer layers (2.5%) which decrease in the middle layers to the minimum value of 1%. Glass fibres did not need the maximum graphene weight in the outer layers which means arbitrarily using the maximum graphene weight in the outer layers for this simulation would not produce the most cost effective design. A similar result, as in Table 3.2.2.3, can be seen for the fibre content with the maximum distribution of 60% in the outer layers and in the middle layers, the minimum of 10%.
The thickness ratio for glass suggests a smaller value in the outer layer, in this case 5%, increasing to the maximum value in the inner layers for 15%. Carbon fibres on the other hand show the maximum (15%) or close to the maximum value in the outer layers which decreased towards the inner layers.

Referring to Figure 3.2.2.4, we can see the fundamental frequency for different stacking sequences produced similar results. For glass fibres the largest range of the fundamental frequency is 0.52% (0.0384 to 0.0386) and for carbon it is 1.08% (0.0550 to 0.0556).

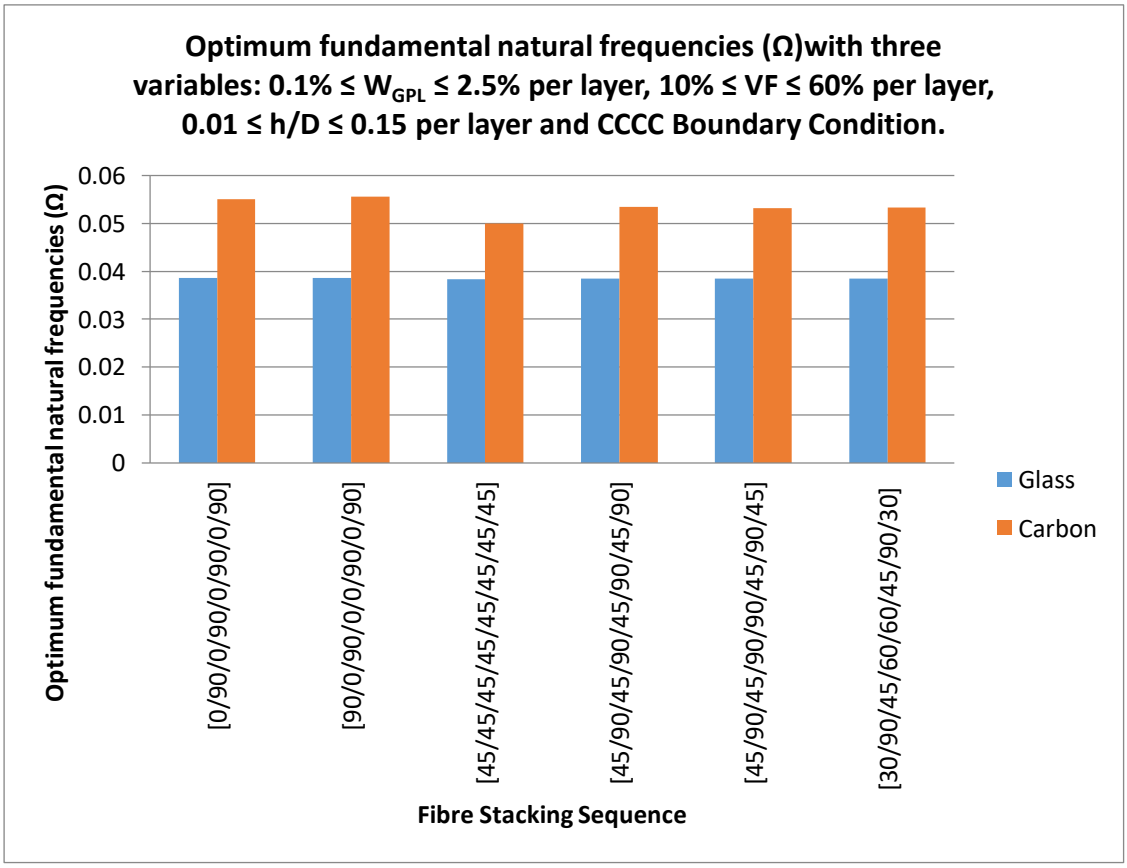

Figure 3.2.2. 4: Graphical representation of result from Table 3.2.2.4

Table 3.2.2. 5: Optimum fundamental natural frequencies (Ω)with three variables: W_{GPL} ,V_F and h/D for CFFF boundary conditions

Stacking sequence		**Optimal W_{GPL}**	**Optimal V_F**	**h_i/D**	**Ω**
		$0.1\% \le W_{GPL} \le 2.5\%$ per layer	$10\% \le V_F \le 60\%$ per layer	$0.01 \le h/D \le 0.15$ per layer	
[0/90/0/90/0/ 90/0/90]	**Glass**	[0.025/0.023/0.001/0.001/ 0.001/0.001/0.023/0.025]	[0.6/0.4/0.1/0.5/ 0.5/0.1/0.4/0.6]	[0.15/0.15/0.15/0.05/ 0.05/0.15/0.15/0.15]	0,0039
	Carbon	[0.025/0.023/0.001/0.001/ 0.001/0.001/0.023/0.025]	[0.6/0.6/0.1/0.5/ 0.5/0.1/0.6/0.6]	[0.15/0.15/0.05/0.15/ 0.15/0.05/0.15/0.15]	0.0058
[90/0/90/0/0/ 90/0/90]	**Glass**	[0.025/0.023/0.001/0.001/ 0.001/0.001/0.023/0.025]	[0.6/0.4/0.1/0.5/ 0.5/0.1/0.4/0.6]	[0.15/0.15/0.12/0.08/ 0.08/0.12/0.15/0.15]	0,0038
	Carbon	[0.006/0.025/0.018/0.001/ 0.001/0.018/0.025/0.006]	[0.6/0.6/0.1/0.5/ 0.5/0.1/0.6/0.6]	[0.05/0.15/0.15/0.15/ 0.15/0.15/0.15/0.05]	0.0061
[45/45/45/45/ 45/45/45/45]	**Glass**	[0.025/0.023/0.001/0.001/ 0.001/0.001/0.023/0.025]	[0.6/0.4/0.1/0.5/ 0.5/0.1/0.4/0.6]	[0.15/0.15/0.15/0.05/ 0.05/0.15/0.15/0.15]	0.0038
	Carbon	[0.025/0.023/0.001/0.001/ 0.001/0.001/0.023/0.025]	[0.6/0.4/0.1/0.5/ 0.5/0.1/0.4/0.6]	[0.15/0.15/0.12/0.08/ 0.08/0.12/0.15/0.15]	0.0041
[45/90/45/90/ 45/90/45/90]	**Glass**	[0.025/0.023/0.001/0.001/ 0.001/0.001/0.023/0.025]	[0.6/0.4/0.1/0.5/ 0.5/0.1/0.4/0.6]	[0.15/0.15/0.13/0.07/ 0.07/0.13/0.15/0.15]	0.0037
	Carbon	[0.025/0.023/0.001/0.001/ 0.001/0.001/0.023/0.025]	[0.6/0.3/0.1/0.5/ 0.5/0.1/0.3/0.6]	[0.15/0.15/0.12/0.08/ 0.08/0.12/0.15/0.15]	0.0036
[45/90/45/90/ 90/45/90/45]	**Glass**	[0.025/0.023/0.001/0.001/ 0.001/0.001/0.023/0.025]	[0.6/0.4/0.1/0.5/ 0.5/0.1/0.4/0.6]	[0.15/0.15/0.13/0.07/ 0.07/0.13/0.15/0.15]	0.0037
	Carbon	[0.025/0.023/0.001/0.001/ 0.001/0.001/0.023/0.025]	[0.6/0.3/0.1/0.5/ 0.5/0.1/0.3/0.6]	[0.15/0.15/0.14/0.06/ 0.06/0.14/0.15/0.15]	0.0040
[30/90/45/60/ 60/45/90/30]	**Glass**	[0.025/0.023/0.001/0.001/ 0.001/0.001/0.023/0.025]	[0.6/0.4/0.1/0.5/ 0.5/0.1/0.4/0.6]	[0.15/0.15/0.15/0.05/ 0.05/0.15/0.15/0.15]	0.0038
	Carbon	[0.025/0.023/0.001/0.001/ 0.001/0.001/0.023/0.025]	[0.6/0.3/0.1/0.5/ 0.5/0.1/0.3/0.6]	[0.15/0.15/0.13/0.07/ 0.07/0.13/0.15/0.15]	0.0050

Note: D/L = 0.1, aspect ratio = 1 and total W_{GPL} of the laminate equal to 10%

The results in Table 3.2.2.5 are for the CFFF (clamped and free) boundary condition. The change from glass to carbon, again, increased the fundamental frequency in a range of 7.5% to 37.70%. This is a much larger range then for the SSSS and CCCC boundary conditions. It is evident that for the [45/90/45/90/45/90/45/90] stacking sequence that the fundamental frequency decreased by 2.78%.

The largest fundamental frequency produced was 0.0061 which utilized carbon fibres with a stacking sequence of [90/0/90/0/0/90/0/90]. The largest fundamental frequency for glass was 0.0039 with the [0/90/0/90/0/90/0/90] stacking sequence. Similar to Table 3.2.2.4 we see for the glass fibres, the fundamental frequency values are almost identical for different stacking sequences.

All simulations in Table 3.2.2.5, except the [90/0/90/0/0/90/0/90] stacking sequence, required the maximum distribution of graphene in the outer layers (2.5%) which decrease in the middle layers to the minimum value of 1%. A similar result, as in Table 3.2.2.3 and Table 3.2.2.4, can be seen for the fibre content with the maximum distribution of 60% in the outer layers and in the middle layers, the minimum of 10%.

The thickness ratio for both glass and carbon fibres suggest the maximum value in the outer layer, in this case 15%, decreasing to a smaller value (5% or almost 5%) in the inner layers.

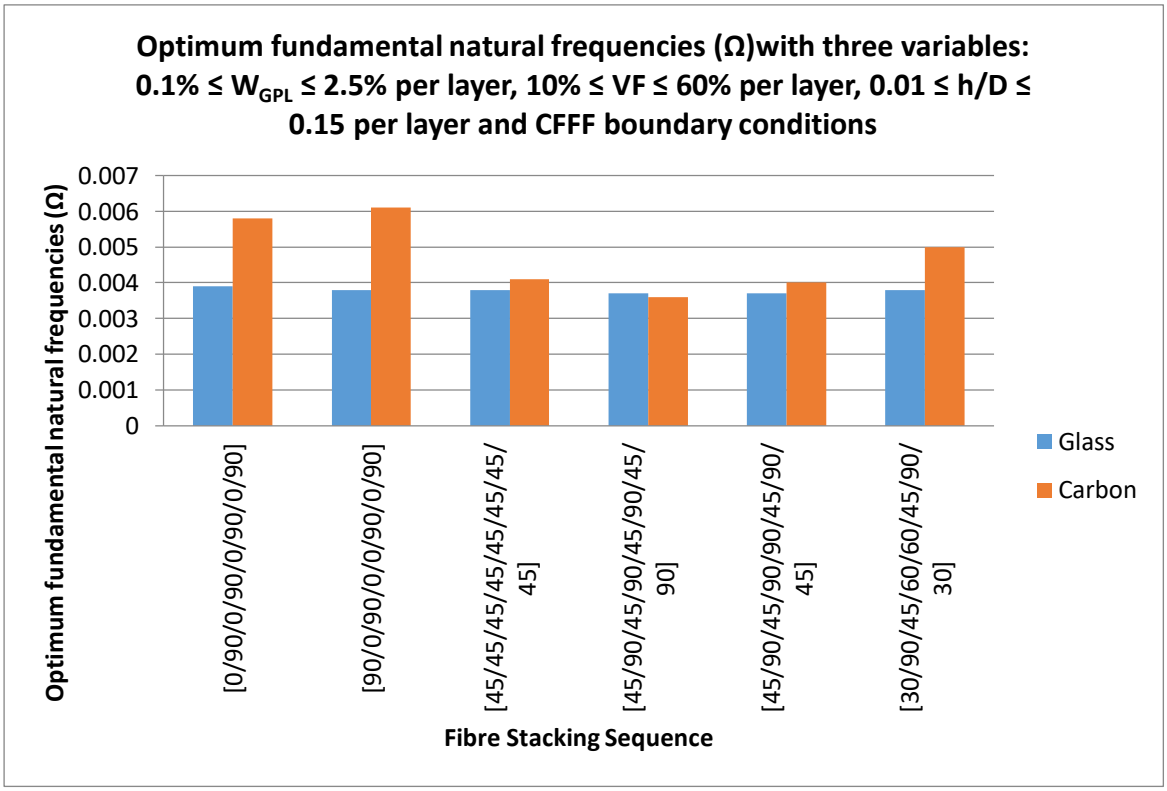

Figure 3.2.2. 5: Graphical representation of result from Table 3.2.2.5

Referring to Figure 3.2.2.5, we can see the fundamental frequency for the [0/90/0/90/0/90/0/90] and [90/0/90/0/0/90/0/90] stacking sequence produced similar results. It is clear from the figure that the optimum fundamental frequency for glass is similar for the different stacking sequences but vary for carbon fibres. For glass fibres the largest range of the fundamental frequency is 5.13% (0.0037 to 0.0039) and for carbon it is 40.98% (0.0036 to 0.0061).

Table 3.2.2. 6: Optimum fundamental natural frequencies (Ω)with three variables: W_{GPL} ,V_F and h/D for SCSC boundary condition

Stacking sequence		**Optimal W_{GPL}**	**Optimal V_F**	**h_i/D**	**Ω**
		$0.1\% \le W_{GPL} \le 2.5\%$ per layer	$10\% \le V_F \le 60\%$ per layer	$0.01 \le h/D \le 0.15$ per layer	
[0/90/0/90/0/ 90/0/90]	**Glass**	[0.015/0.025/0.009/0.001/ 0.001/0.009/0.025/0.015]	[0.6/0.6/0.6/0.1/ 0.1/0.6/0.6/0.6]	[0.05/0.15/0.15/0.15/ 0.15/0.15/0.15/0.05]	0.0309
	Carbon	[0.025/0.023/0.001/0.001/ 0.001/0.001/0.023/0.025]	[0.6/0.6/0.6/0.1/ 0.1/0.6/0.6/0.6]	[0.12/0.15/0.08/0.15/ 0.15/0.08/0.15/0.12]	0.0435
[90/0/90/0/0/ 90/0/90]	**Glass**	[0.015/0.025/0.009/0.001/ 0.001/0.009/0.025/0.015]	[0.6/0.6/0.6/0.1/ 0.1/0.6/0.6/0.6]	[0.05/0.15/0.15/0.15/ 0.15/0.15/0.15/0.05]	0.0307
	Carbon	[0.007/0.025/0.017/0.001/ 0.001/0.017/0.025/0.007]	[0.6/0.6/0.1/0.1/ 0.1/0.1/0.6/0.6]	[0.05/0.15/0.15/0.15/ 0.15/0.15/0.15/0.05]	0.0442
[45/45/45/45/ 45/45/45/45]	**Glass**	[0.015/0.025/0.009/0.001/ 0.001/0.009/0.025/0.015]	[0.6/0.6/0.6/0.1/ 0.1/0.6/0.6/0.6]	[0.05/0.15/0.15/0.15/ 0.15/0.15/0.15/0.05]	0.0310
	Carbon	[0.025/0.023/0.001/0.001/ 0.001/0.001/0.023/0.025]	[0.6/0.6/0.6/0.1/ 0.1/0.6/0.6/0.6]	[0.15/0.15/0.05/0.15/ 0.15/0.05/0.15/0.15]	0.0405
[45/90/45/90/ 45/90/45/90]	**Glass**	[0.015/0.025/0.009/0.001/ 0.001/0.009/0.025/0.015]	[0.6/0.6/0.6/0.1/ 0.1/0.6/0.6/0.6]	[0.05/0.15/0.15/0.15/ 0.15/0.15/0.15/0.05]	0.0306
	Carbon	[0.025/0.023/0.001/0.001/ 0.001/0.001/0.023/0.025]	[0.6/0.6/0.1/0.1/ 0.1/0.1/0.6/0.6]	[0.15/0.15/0.05/0.15/ 0.15/0.05/0.15/0.15]	0.0380
[45/90/45/90/ 90/45/90/45]	**Glass**	[0.025/0.023/0.001/0.001/ 0.001/0.001/0.023/0.025]	[0.6/0.6/0.1/0.1/ 0.1/0.1/0.6/0.6]	[0.15/0.15/0.15/0.05/ 0.05/0.15/0.15/0.15]	0.0323
	Carbon	[0.025/0.023/0.001/0.001/ 0.001/0.001/0.023/0.025]	[0.6/0.6/0.6/0.1/ 0.1/0.6/0.6/0.6]	[0.15/0.15/0.05/0.15/ 0.15/0.05/0.15/0.15]	0.0395
[30/90/45/60/ 60/45/90/30]	**Glass**	[0.025/0.023/0.001/0.001/ 0.001/0.001/0.023/0.025]	[0.6/0.6/0.1/0.1/ 0.1/0.1/0.6/0.6]	[0.15/0.15/0.15/0.05/ 0.05/0.15/0.15/0.15]	0.0325
	Carbon	[0.025/0.006/0.018/0.001/ 0.001/0.018/0.006/0.025]	[0.6/0.6/0.6/0.1/ 0.1/0.6/0.6/0.6]	[0.15/0.05/0.15/0.15/ 0.15/0.15/0.05/0.15]	0.0437

Note: D/L = 0.1, aspect ratio = 1 and total W_{GPL} of the laminate equal to 10%

The results in Table 3.2.2.6 are for the SCSC (simply supported and clamped) boundary condition.
The change from glass to carbon, as seen in Tables 3.2.2.3 to 3.2.2.5, increased the fundamental frequency. The range of increase is 18.23% to 30.54%.

The largest fundamental frequency produced for carbon fibres was 0.0437 with a stacking sequence of [30/90/45/60/60/45/90/30]. The largest fundamental frequency for glass was 0.031 with the [45/45/45/45/45/45/45/45] stacking sequence. As seen previously the fundamental frequency resulting from the glass fibres are similar.

In Table 3.2.2.6 the amount of graphene needed in the layers differs for the various stacking sequences. Carbon fibres for all cases except the [90/0/90/0/0/90/0/90] stacking sequence required the maximum value of 2.5% in the outer layers. However, glass fibres only required the maximum graphene content in the outer layers for the [45/90/45/90/90/45/90/45] and [30/90/45/60/60/45/90/30] stacking sequences. A similar result, as in Table 3.2.2.3 to 3.2.2.5, can be seen for the fibre content with the maximum distribution of 60% in the outer layers and in the middle layers, the minimum of 10%.

The thickness ratio for both glass and carbon fibres vary for different stacking sequences. The stacking sequences [45/90/45/90/90/45/90/45] and [30/90/45/60/60/45/90/30] resulted in the maximum value of 15% for the thickness ratio in the outer layers. In this simulation, these two stacking sequenced required the maximum amounts of graphene, fibre and thickness ratio in the outer layers.

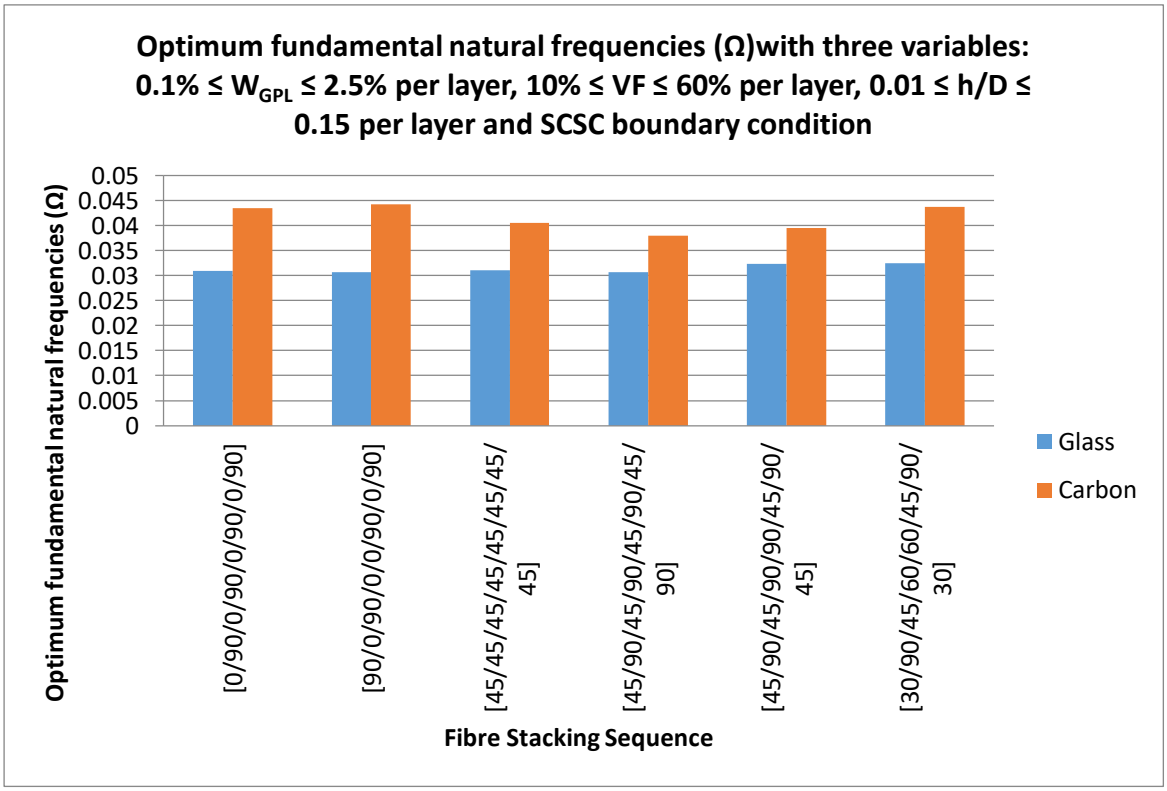

Figure 3.2.2. 6: Graphical representation of result from Table 3.2.2.6

Referring to Figure 3.2.2.6, it is clear that the optimum fundamental frequency for glass is similar for the different stacking sequences but vary for carbon fibres. For glass fibres the largest variance of the fundamental frequency is 1.29% (0.0306 to 0.031) and for carbon it is 13.04% (0.038 to 0.0437).

By a careful study of Tables 3.2.2.3 to 3.2.2.6, it is noticed that a unified conclusion cannot be attained for the optimal quantities which are derived from the different boundary conditions, fibre types and stacking sequences.

There are however some comments that characterized more than one cases of the presented output. For most of the different boundary conditions, stacking sequences and fibre types, the optimal distribution of thickness ratio is the one with the maximum value in the outer layers.

Analysis of the graphene weight shows for the majority of results the optimum distribution is a maximum value (2.5%) at the outer layers whilst the inner layers decrease in graphene content.

For glass fibres in CCCC or SCSC boundary conditions this is not observed, since the value of the thickness ratio assigned is not the maximum allowable value in the outer layers. For these simulations, the graphene weight is not assigned the maximum value in the outer layers. Furthermore, for the majority of the cases, optimal fibre (glass or carbon) distribution results in maximum values at the outer layers. The CFFF boundary condition shows that the optimal fibre distribution is maximum values (60%) at the outer layers and decreasing inward until increasing again in the middle two layers (to 50%).

The maximum optimal frequencies obtained from each boundary condition type, depend on the stacking sequence and fibre type. But a unique trend is not observed from the tested angle fibre distributions.

In the results shown in Table 3.2.2.7 the fibre angles have been added as design variables, thus, the models consider three variables, namely the graphene weight, the fibre content and the fibre angle relative to the x-axis.

Table 3.2.2. 7: Optimum fundamental natural frequencies (Ω) with three variables: W_{GPL}, V_F and fibre angle

Boundary conditions		**Optimal W_{GPL}**	**Optimal V_F**	**Fibre angle ϑ (°)**	**Ω**
		$0.1\% \leq W_{GPL} \leq 2.5\%$ per layer	$10\% \leq VF \leq 60\%$ per layer	fibre angle between -90° and 90°.	
SSSS	**Glass**	[0.025/0.023/0.001/0.001/ 0.001/0.001/0.023/0.025]	[0.6/0.6/0.1/0.1/ 0.1/0.1/0.6/0.6]	[-45/44/45/47/ 47/45/44/-45]	0.1894
	Carbon	[0.025/0.015/0.009/0.001/ 0.001/0.009/0.015/0.025]	[0.6/0.6/0.6/0.1/ 0.1/0.6/0.6/0.6]	[-45/45/45/46/ 46/45/45/-45]	0.2677
CCCC	**Glass**	[0.025/0.023/0.001/0.001/ 0.001/0.001/0.023/0.025]	[0.6/0.6/0.1/0.1/ 0.1/0.1/0.6/0.6]	[90/-1/90/-89/ -89/90/-1/90]	0.3135
	Carbon	[0.021/0.011/0.01/0.008/ 0.008/0.01/0.011/0.021]	[0.6/0.6/0.6/0.6/ 0.6/0.6/0.6/0.6]	[90/0/90/-90/ -90/90/0/90]	0.3939
CFFF	**Glass**	[0.023/0.025/0.001/0.001/ 0.001/0.001/0.025/0.023]	[0.6/0.6/0.1/0.1/ 0.1/0.1/0.6/0.6]	[1/88/2/87/ 87/2/88/1]	0.0349
	Carbon	[0.023/0.025/0.001/0.001/ 0.001/0.001/0.025/0.023]	[0.6/0.1/0.6/0.1/ 0.1/0.6/0.1/0.6]	[1/88/2/87/ 87/2/88/1]	0.0601
SCSC	**Glass**	[0.025/0.023/0.001/0.001/ 0.001/0.001/0.023/0.025]	[0.6/0.6/0.1/0.1/ 0.1/0.1/0.6/0.6]	[2/0/0/-19/ -19/0/0/2]	0.2612
	Carbon	[0.019/0.013/0.01/0.008/ 0.008/0.01/0.013/0.019]	[0.6/0.6/0.6/0.6/ 0.6/0.6/0.6/0.6]	[0/-1/-1/1/ 1/-1-1/0]	0.3629

Note: D/L = 0.1, aspect ratio = 1 and total W_{GPL} of the laminate equal to 10%

Results indicate that the optimal natural vibration is obtained for different optimal stacking sequences, for the tested boundary conditions. For all the cases, a higher graphene weight in the outer layers which decreases towards the middle layers, results in the optimal reinforcing distribution. The distribution of glass fibres in all boundary conditions show that the maximum allowable fibre distribution in the outer layers and decreasing towards the inner layers is one factor contributing to the optimum fundamental frequency.

For carbon fibres in the CCCC and SCSC boundary conditions, the optimum fundamental frequency is obtained for maximum fibre content in all layers, while for CFFF, an irregular carbon fibre distribution with maximum values in the outer and middle layers is obtained.

A noticeable trend in the fibre angle is that for each boundary condition, very similar or the same fibre angles are obtained for glass and carbon fibres. Therefore, in this test the fibre angle is not a significant factor in the optimum fundamental frequency when comparing the results of glass vs. carbon.

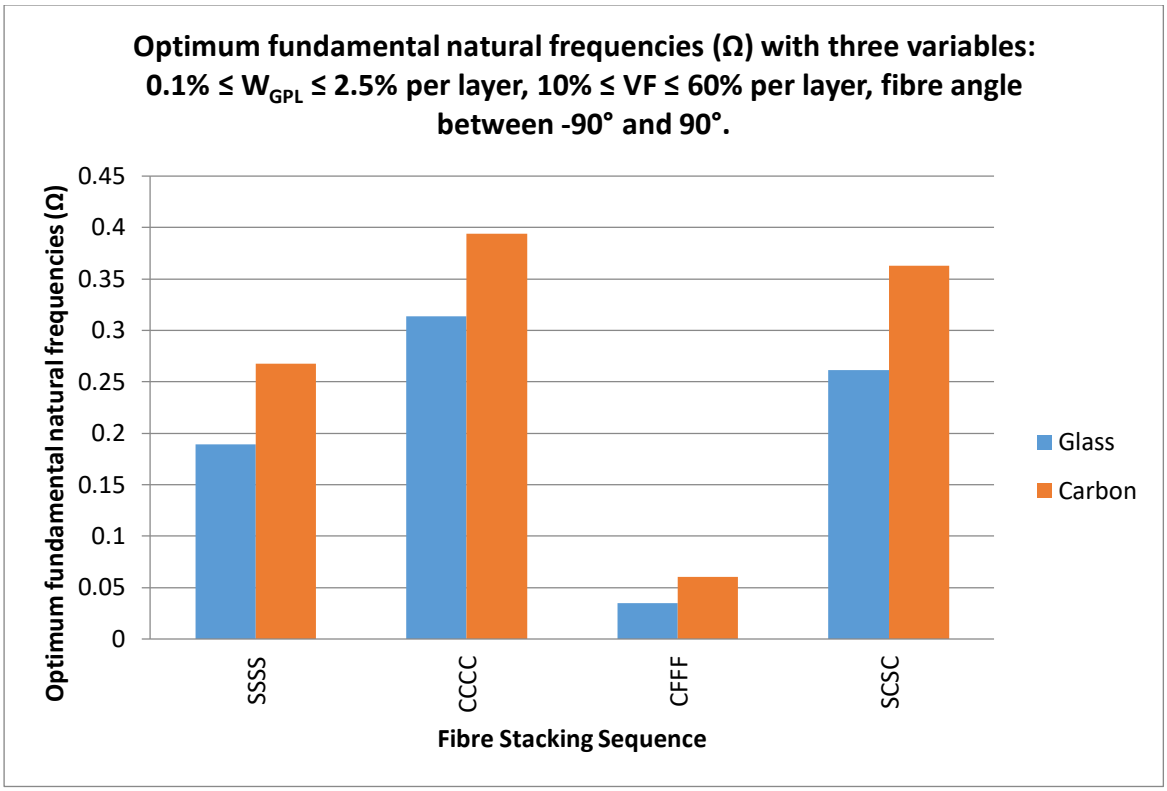

Figure 3.2.2. 7: Graphical representation of result from Table 3.2.2.7

Figure 3.2.2.7 shows the comparison of the optimum fundamental frequency, for the four boundary conditions and two fibre types, in a graph format. The graph shows us that CCCC and SCSC have close values for the optimum fundamental frequency followed closely by SSSS. The boundary condition CFFF however, has much lower values than the other three. This has been a noticeable trend in the simulations studied in this thesis.

CHAPTER 4: CONCLUSION

The natural frequency for a hybrid, multi-scale graphene/fibre reinforced composite laminate plate is studied in this thesis. There is a possibility this study could aid industries, such as aerospace, in increasing the natural frequency of nanocomposite structures in order to lower the possibility of resonance occurring. The laminate is defined as a 3-phase nanocomposite plate consisting of fibres, a polymer matrix and graphene nanoplatelets. The main goal of this work is to study the vibration response of this innovative formulation, where in the traditional fibre reinforced composite laminate that utilizes glass or carbon fibre, nanocomposite (graphene) reinforcement has been considered. Towards the optimal, cost-effective design of the laminate, the optimum distribution of the constituent materials along the thickness of the structure is investigated.

An optimization numerical algorithm is applied to the laminate to produce the most efficient natural frequency. The maximum fundamental frequency is required to avoid resonance. The natural vibration problem is solved in the framework of the finite element method, using a First Order Shear Deformation theory (FSDT). Four boundary conditions are applied to the laminate plate to record various changes in the optimized natural frequency. Micromechanics equations are used to calculate the effective properties of the composite structure.

An important result of this research is to determine the optimal graphene weight for each layer, required to optimize the natural frequency of the structure. An 8-layer laminate plate is formulated and several optimization problems are defined, using different variables.

The first simulation considers only graphene weight as the single variable of the problem. Results indicated that the maximum allowable quantity of graphene, 10% for all layers as shown in Table 3.2.1.1 and 2.5% as shown in Table 3.2.1.2, is required to produce the optimum natural frequency, which is expected.

When a restriction for the overall allowable graphene weight is posed (Table 3.2.1.3), it is observed that the outer layers of the plate require a larger quantity of graphene than that of the inner layers to produce the optimum fundamental frequency.

For the SSSS boundary condition the outer layer required 25 times more graphene than the inner layer for both glass and carbon fibers. The CCCC boundary condition showed the outer layers required 15 times more graphene for glass and 25 times more for carbon fibre. CFFF showed 25 times more graphene needed in the outer layers than inner layers for both glass and carbon fibre. Lastly, the SCSC boundary condition required 15 times more graphene in the outer layer than in the inner for glass and 25 times more for carbon fibre.

From Table 3.2.1.4 and 3.2.1.5, the increase in total laminate thickness over edge length (D/L ratio) results in an expected increase in the fundamental frequency of the laminate. Furthermore, increasing the aspect ratio, as in Table 3.2.1.6, leads to higher fundamental frequencies and a similar distribution of graphene in the inner and outer layers as seen previously, where, the outer layers required a larger amount of graphene than the inner layers.

When a different value for the minimum allowable graphene weight is tested (0.1% to 2.5% and 1% to 2.5%) in Table 3.2.1.7, the model using the lower minimum value leads to a higher fundamental frequency, accompanied by a higher graphene weight for the two outer layers of the laminate. Thus, a better distribution of the nano-reinforcement on the laminate is achieved in this case.

The optimum fundamental frequency for varying graphene and fibre content has also been analyzed in Table 3.2.2.1. The results indicate that the boundary conditions in this case play a significant role in the magnitude of the optimum fundamental frequency. The CCCC boundary condition resulted in the highest optimum fundamental frequencies of 0.3135 and 0.3913 for glass and carbon fibres respectively. Table 3.2.2.1 shows that, for carbon fibres, the change in boundary condition results in different fibre contents required to optimize the composite. For example the SSSS, CCCC, CFFF and SCSC boundary conditions required 10%, 60%, 30% and 60% fibre content in the middle layers.

It can be seen in Tables 3.2.2.3 to 3.2.2.6 that the differing factor in these cases was the boundary conditions. Boundary condition CCCC displayed the largest optimum fundamental frequencies in comparison to the others with SCSC being the second largest, then SSSS having the third largest optimum fundamental frequencies and

finally CFFF having the smallest (see Figure 3.2.2.3 to Figure 3.2.2.6). Additionally, adopting the maximum fibre content (60%) and/or graphene weight (2.5%) per layer does not always lead to the optimum fundamental frequency for the laminate.

A simulation for zero graphene in a laminate is also tested where fibre content is the variable (Table 3.2.2.2). It is evident from the resultant natural frequency values that the optimal natural vibrations are reduced in a range between 9% and 39% when no graphene is used in the laminate. This indicates that the addition of even a small quantity of graphene (as tested in this work) can bring a significant improvement of the natural vibration response of the laminate.

In another investigation, the thickness ratio is considered as a variable of the optimization function. For most of the tested cases, it is evident that the optimal distribution of thickness ratio is the one with the maximum value in the outer layers. No physical explanation was found for this. Future studies could be done to determine the reason behind this finding. This cannot however be extended to glass fibres with CCCC or SCSC boundary conditions as the maximum thickness ratio does not appear to be in the outer layers. The optimal fibre distribution also shows the maximum allowable values for fibre content (60%) required at more than just the two outer layers of the composite but the CFFF boundary condition required the maximum fibre content at the two outer most layers only.

A final study is carried out by selecting graphene weight, fibre content and fibre angles as variables of the optimization. For this test, higher graphene and fibre content appearing in the outer layers was the output of the optimization analysis. The higher reinforcement in the outer layers produced the optimal fundamental frequency but for carbon fibres with CCCC or SCSC boundary conditions, maximum fibre content (60%) in all layers results in the optimum fundamental frequency. For the CFFF boundary condition, an irregular carbon fibre distribution is obtained.

To answer the research question set out at the beginning of this thesis: “How could the use of graphene as a nano-reinforcment optimize the vibrational response of a composite laminate?”

The majority of results obtained in the various studies conducted show that graphene can be added to composite materials, as nano-reinforcement, to increase the

optimum fundamental frequency. It is important to note that the optimal distribution is not always the maximum content for all layers. Utilizing the optimum quantities as presented in this study, could produce a more cost effective composite. It is also noted that for most cases, the outer layers can be used to maximize the fundamental frequency as the maximum values of the constituent materials are found in the outer layers with decreasing amount closer to the middle layers.

Future steps of this research include the investigation of functionally graded nano-materials, where the graphene weight varies along the thickness of the laminate, following a pre-defined distribution. In addition, a non-constant graphene distribution along each layer may also result in an improved response and cost-effective usage of the material. By using a non-constant graphene distribution, we may be able to reinforce the critical zones of each layer. As a result this would decrease the amount of graphene needed to attain the optimum fundamental frequency and make the nanocomposite more cost-effective. These ideas are left for future investigation.

REFERENCES

[1] Elmarakbi, A., Karagiannidis, P., Ciappa, A., Innocente, F., Galise, F., Martorana, B., Gómez, J. (2019). 3-phase hierarchical graphene-based epoxy nanocomposite laminates for automotive applications. Journal of Materials Science & Technology. doi:10.1016/j.jmst.2019.05.033

[2] Liu, H., & Brinson, L. C. (2008). Reinforcing efficiency of nanoparticles: A simple comparison for polymer nanocomposites. Composites Science and Technology, 68(6), 1502–1512. doi:10.1016/j.compscitech.2007.10.033

[3] Kayikci, R. & Sonmez, F. O. (2011). Design of composite laminates for optimum frequency response. Journal of Sound and Vibration 331, 1759-1776. doi:10.1016/j.jsv.2011.12.020

[4] Gandomkar, F A, Wan Badaruzzaman, W H, Osman, S A, & Ismail, A. (2013). Experimental and numerical investigation of the natural frequencies of the composite profiled steel sheet dry board (PSSDB) system. Journal of the South African Institution of Civil Engineering, 55(1), 11-21. Retrieved March 29, 2020, from http://www.scielo.org.za/scielo.php?script=sci_arttext&pid=S1021-20192013000100002&lng=en&tlng=en.

[5] Ribes, F. & Velarte Gonzalez, Jose Luis & Luis Perez-Garnes, Jose & Irene Real-Herráiz, Julia. (2016). Study of Vibrations in a Short-Span Bridge Under Resonance Conditions Considering Train-Track Interaction. Latin American Journal of Solids and Structures. 13. 1236-1249. 10.1590/1679-78252773.

[6] Ewins, D. J. (2010). Control of vibration and resonance in aero engines and rotating machinery – An overview. International Journal of Pressure Vessels and Piping, 87(9), 504–510. doi:10.1016/j.ijpvp.2010.07.001

[7] Rafiee, M. A., Rafiee, J., Wang, Z., Song, H., Yu, Z.-Z., & Koratkar, N. (2009). Enhanced Mechanical Properties of Nanocomposites at Low Graphene Content. ACS Nano, 3(12), 3884–3890. doi:10.1021/nn9010472

[8] Mohseni, A., & Shakouri, M. (2020). Natural frequency, damping and forced responses of sandwich plates with viscoelastic core and graphene nanoplatelets reinforced face sheets. Journal of Vibration and Control, 107754631989345. doi:10.1177/1077546319893453

[9] Shi, G., Araby, S., Gibson, C. T., Meng, Q., Zhu, S., & Ma, J. (2018). Graphene Platelets and Their Polymer Composites: Fabrication, Structure, Properties, and Applications. Advanced Functional Materials, 28(19), 1-44, 1706705. doi:10.1002/adfm.201706705

[10] Cataldi, P., Athanassiou, A., & Bayer, I. (2018). Graphene Nanoplatelets-Based Advanced Materials and Recent Progress in Sustainable Applications. Applied Sciences, 8(9), 1-35, 1438. doi:10.3390/app8091438

[11] Zhu, Z. (2017). An Overview of Carbon Nanotubes and Graphene for Biosensing Applications. Nano-Micro Letters, 9(3), 1-25. doi:10.1007/s40820-017-0128-6

[12] Choi, W., Lahiri, I., Seelaboyina, R., & Kang, Y. S. (2010). Synthesis of Graphene and Its Applications: A Review. Critical Reviews in Solid State and Materials Sciences, 35(1), 52-71.

[13] Qiu, J., & Wang, S. (2010). Enhancing polymer performance through graphene sheets. Journal of Applied Polymer Science, 119(6), 3670–3674.

[14] Feng, Z., Li, Y., Tang, D., Xin, C., Xiong, W., & Zhang, H. (2019). Fabrication of Graphene-Reinforced Nanocomposites with Improved Fracture Toughness in Net Shape for Complex 3D Structures via Digital Light Processing, Graphene-Reinforced Polymer Nanocomposites, 5, 1-16.

[15] Thai, C. H., Ferreira, A. J. M., Tran, T. D., & Phung-Van, P. (2019). Free vibration, buckling and bending analyses of multilayer functionally graded graphene nanoplatelets reinforced composite plates using the NURBS formulation. Composite Structures 220, 1-26.

[16] Mohamad, N., Yaakub, J., Ab Maulod, H. E., Jeefferie, A. R., Yuhazri, M. Y., Lau, K. T., et al. (2017). Vibrational damping behaviors of graphene nanoplatelets reinforced NR/EPDM nanocomposites, Journal of Mechanical Engineering and Sciences,11, 3274-3287.

[17] Shen, H.-S., Lin, F., & Xiang, Y. (2017). Nonlinear vibration of functionally graded graphene-reinforced composite laminated beams resting on elastic foundations in thermal environments. Nonlinear Dynamics, 90(2), 899-914. doi:10.1007/s11071-017-3701-0

[18] Zhang, Z., Li, Y., Wu, H., Zhang, H., Wu, H., Jiang, S., & Chai, G. (2018). Mechanical analysis of functionally graded graphene oxide-reinforced composite beams based on the first-order shear deformation theory. Mechanics of Advanced Materials and Structures, 1–9. doi:10.1080/15376494.2018.1444216

[19] Shahrjerdi, A., & Yavari, S. (2018). Free vibration analysis of functionally graded graphene-reinforced nanocomposite beams with temperature-dependent properties. Journal of the Brazilian Society of Mechanical Sciences and Engineering, 1-13.

[20] Narita, Y. (2003). Layerwise optimization for the maximum fundamental frequency of laminated composite plates. Journal of Sound and Vibration, 263(5), 1005–1016.

[21] Pashmforoush, F. (2019). Statistical analysis on free vibration behavior of functionally graded nanocomposite plates reinforced by graphene platelets. Composite Structures. doi:10.1016/j.compstruct.2019.01.066

[22] Feng, C., Kitipornchai, S., & Yang, J. (2017). Nonlinear free vibration of functionally graded polymer composite beams reinforced with graphene nanoplatelets (GPLs). Engineering Structures, 140, 110–119. doi:10.1016/j.engstruct.2017.02.052

[23] Young, R. J., Liu, M., Kinloch, I. A., Li, S., Zhao, X., Vallés, C., & Papageorgiou, D. G. (2018). The mechanics of reinforcement of polymers by graphene nanoplatelets. Composites Science and Technology, 154, 110–116. doi:10.1016/j.compscitech.2017.11.007

[24] Atif, R., Shyha, I., & Inam, F. (2016). Mechanical, Thermal, and Electrical Properties of Graphene-Epoxy Nanocomposites—A Review. Polymers, 8(8), 281. doi:10.3390/polym8080281

[25] Shahil, K. M., & Balandin, A. A. (2011). Graphene –Based Nanocomposites as Highly Efficient Thermal Interface Materials. 1-18.

[26] Song, M., Kitipornchai, S., & Yang, J. (2017). Free and forced vibrations of functionally graded polymer composite plates reinforced with graphene nanoplatelets. Composite Structures, 159, 579–588. doi:10.1016/j.compstruct.2016.09.070

[27] M. Rafiee, F. Nitzsche, M.R. Labrosse (2018). Modeling and mechanical analysis of multiscale fiber-reinforced graphene composites: Nonlinear bending, thermal post-buckling and large amplitude, International Journal of Non-Linear Mechanics 103, 104-112

[28] O. Aluko, S. Gowtham, G. M. Odegard (2017). Multiscale modeling and Analysis of Graphene Nanoplatelet /Carbon Fiber/Epoxy Hybrid Composite, Composites Part B: Engineering, 131, Pages 82-90

[29] Pin-Ning Wang, Tsung-Han Hsieh, Chin-Lung Chiang, Ming-Yuan Shen (2015). Synergetic Effects of Mechanical Properties on Graphene Nanoplatelet and Multiwalled Carbon Nanotube Hybrids Reinforced

Epoxy/Carbon Fiber Composites, Journal of Nanomaterials Volume 2015, Article ID 838032, 9 pages

[30] Weikang Li, Anthony Dichiara, Jinbo Bai (2013). Carbon nanotube–graphene nanoplatelet hybrids as high-performance multifunctional reinforcements in epoxy composites, Composites Science and Technology, 74, 221-227

[31] M. Ahmadi, R. Ansari, H. Rouhi (2017). Multi-scale bending, buckling and vibration analyses of carbon fiber/carbon nanotube-reinforced polymer nanocomposite plates with various shapes, Physica E: Low-dimensional Systems and Nanostructures, 93, 17-25

[32] Raheb Gholami, Reza Ansari, Yousef Gholami (2018). Numerical study on the nonlinear resonant dynamics of carbon nanotube/fiber/polymer multiscale laminated composite rectangular plates with various boundary conditions, Aerospace Science and Technology 78, 118-129

[33] J. Seidi, S. Kamarian (2017). Free vibrations of non-uniform CNT/fiber/polymer nanocomposite beams, Curved and Layered Structures 4, 21-30

[34] Radebe, I. S., Drosopoulos, G. A., & Adali, S. (2019). Buckling of non-uniformly distributed graphene and fibre reinforced multiscale angle-ply laminates. Meccanica. doi:10.1007/s11012-019-01067-3

[35] Ho-Huu, V., Do-Thi, T. D., Dang-Trung, H., Vo-Duy, T., & Nguyen-Thoi, T. (2016). Optimization of laminated composite plates for maximizing buckling load using improved differential evolution and smoothed finite element method. Composite Structures, 146, 132–147. doi:10.1016/j.compstruct.2016.03.016

[36] An, H., Chen, S., & Huang, H. (2018). Maximization of fundamental frequency and buckling load for the optimal stacking sequence design of laminated composite structures. Proceedings of the Institution of Mechanical Engineers,

Part L: Journal of Materials: Design and Applications, 146442071876502. doi:10.1177/1464420718765020

[37] Kayikci, R., & Sonmez, F. O. (2012). Design of composite laminates for optimum frequency response. Journal of Sound and Vibration, 331(8), 1759–1776. doi:10.1016/j.jsv.2011.12.020

[38] M. Kemal Apalak, Dervis Karaboga & Bahriye Akay (2014) The Artificial Bee Colony algorithm in layer optimization for the maximum fundamental frequency of symmetrical laminated composite plates, Engineering Optimization, 46:3, 420-437, DOI: 10.1080/0305215X.2013.776551

[39] Sadr, M. H., & Ghashochi Bargh, H. (2011). Optimization of laminated composite plates for maximum fundamental frequency using Elitist-Genetic algorithm and finite strip method. Journal of Global Optimization, 54(4), 707–728. doi:10.1007/s10898-011-9787-x

[40] Kamarian, S., Shakeri, M., & Yas, M. H. (2016). Natural frequency analysis and optimal design of CNT/fiber/polymer hybrid composites plates using mori-tanaka approach, GDQ technique, and firefly algorithm. Polymer Composites, 39(5), 1433–1446. doi:10.1002/pc.24083

[41] Kamarian, S., Shakeri, M., Karimi, B., & Pourasghar, A. (2015). Free vibration analysis and design optimization of nanocomposite-laminated beams using various higher order beam theories and imperialist competitive algorithm. Polymer Composites, 37(8), 2442–2451. doi:10.1002/pc.23429

[42] Reddy JN, Mechanics of Laminated Composite Plates and Shells, 2nd ed. CRC Press 2004

[43] Huang, Y., Yang, Z., Liu, A., & Fu, J. (2018). Nonlinear Buckling Analysis of Functionally Graded Graphene Reinforced Composite Shallow Arches with Elastic Rotational Constraints under Uniform Radial Load. Materials, 11(6), 910. doi:10.3390/ma11060910

[44] Song, M., Yang, J., Kitipornchai, S., & Zhu, W. (2017). Buckling and postbuckling of biaxially compressed functionally graded multilayer graphene nanoplatelet-reinforced polymer composite plates. International Journal of Mechanical Sciences, 131-132, 345–355. doi:10.1016/j.ijmecsci.2017.07.017

[45] Wang Y, Feng C, Zhao Z, Yang J (2018) Eigenvalue buckling of functionally graded cylindrical shells reinforced with graphene platelets (gpl).Compos Structures 202:38-46

[46] Wang, Y., Feng, C., Zhao, Z., & Yang, J. (2018). Buckling of Graphene Platelet Reinforced Composite Cylindrical Shell with Cutout. International Journal of Structural Stability and Dynamics, 18(03), 1850040:1-17. doi:10.1142/s0219455418500402

[47] Vo-Duy, T., Ho-Huu, V., Do-Thi, T. D., Dang-Trung, H., & Nguyen-Thoi, T. (2017). A global numerical approach for lightweight design optimization of laminated composite plates subjected to frequency constraints. Composite Structures, 159, 646–655. doi:10.1016/j.compstruct.2016.09.059

[48] Numerical Optimization. (2006). Springer Series in Operations Research and Financial Engineering. doi:10.1007/978-0-387-40065-5

[49] MATLAB. (2016). version 9.0.0.341360 (R2016a). Natick, Massachusetts: The MathWorks Inc.

[50] Gill, P.E., W. Murray, and M.H. Wright, Numerical Linear Algebra and Optimization, Vol. 1, Addison Wesley, 1991.

[51] Guo, H., Cao, S., Yang, T., & Chen, Y. (2018). Vibration of laminated composite quadrilateral plates reinforced with graphene nanoplatelets using the element-free IMLS-Ritz method. International Journal of Mechanical Sciences, 142-143, 610–621. doi:10.1016/j.ijmecsci.2018.05.029

[52] Guo, H., Cao, S., Yang, T., Chen, Y. (2018). Vibration of laminated composite quadrilateral plates reinforced with graphene nanoplatelets using the element-free IMLS-Ritz method. International Journal of Mechanical Sciences 142–143: 610-621.